Chen *et al. Surface Science and Technology* (2023) 1:13
https://doi.org/10.1007/s44251-023-00013-6

Surface Science and Technology

REVIEW Open Access

# Progress and challenges in energy storage and utilization via ammonia

Chongqi Chen[1], Yanliang Zhou[1], Huihuang Fang[1], Xiaobo Peng[1] and Lilong Jiang[1*]

**Abstract**

Ammonia is a premium energy carrier with high content of hydrogen. However, energy storage and utilization via ammonia still confront multiple challenges. Here, we review recent progress and discuss challenges for the key steps of energy storage and utilization via ammonia (including hydrogen production, ammonia synthesis and ammonia utilization). In hydrogen production, we focus on important processes and catalytic designs for conversion of carbon feedstocks and water into hydrogen. To reveal crucial challenges of ammonia synthesis, catalytic designs and mechanisms are summarized and analyzed, in thermocatalytic synthesis, electrocatalytic synthesis and photocatalytic synthesis of ammonia. Further, in ammonia utilization, important processes and catalytic designs are outlined for ammonia decomposition, ammonia fuel cells and ammonia combustion. The goal of this review is to stimulate development of low-cost and eco-friendly ways for energy storage and utilization via ammonia.

**Keywords** Energy storage, Hydrogen production, Ammonia synthesis, Ammonia utilization

## 1 Introduction

Ammonia ($NH_3$) is a colorless gas with pungent odor and low toxicity, and has been widely used in production of agricultural fertilizers and industrial chemicals. It has also attracted more and more attention in field of renewable energy sources, as an energy carrier [1, 2], because it possesses a high content of hydrogen (> 17 wt.%). In recent decades, a large number of scientists and researchers have been devoted to exploring high-efficiency production of ammonia [3–5]. However, its industrial production is still dominated by Haber–Bosch (HB) process. At present, the HB process has consumed 1 ~ 2% of global energy, accompanying with > 1% of global $CO_2$ emissions [6, 7]. The huge energy consumption and serious environmental pollution are urging us to minimize the cost and pollution of ammonia synthesis, and develop new approaches towards ammonia utilization.

*Correspondence:
Lilong Jiang
jll@fzu.edu.cn
[1] National Engineering Research Center of Chemical Fertilizer Catalyst, Fuzhou University, Fuzhou 350002, Fujian, China

To directly reduce the cost and pollution of ammonia synthesis in HB process, optimization of hydrogen production is an effective strategy. It is well recognized that the HB process employs nitrogen and hydrogen as feedstocks. It is easy to obtain nitrogen from air, but hydrogen production is a high-energy-consumption and/or high-pollution process [8, 9]. In view of the current situation, hydrogen production of HB process mainly utilizes carbon feedstocks (Fig. 1). The carbon feedstocks include hydrocarbons, coal, biomass, etc. [10–12]. Moreover, to minimize environmental pollution, water can also be used as an environmentally friendly feedstock for hydrogen production [13–15]. To date, hydrogen production has been studied extensively, based on the carbon feedstocks and water. It is highly desirable to outline the important processes and catalytic designs of hydrogen production in recent years, to further promote optimization of HB process.

After optimization of hydrogen production, it is important to upgrade ammonia synthesis for further reducing the cost and pollution. In general, the methods of ammonia synthesis are classified into three main categories, i.e., thermocatalytic synthesis, electrocatalytic synthesis

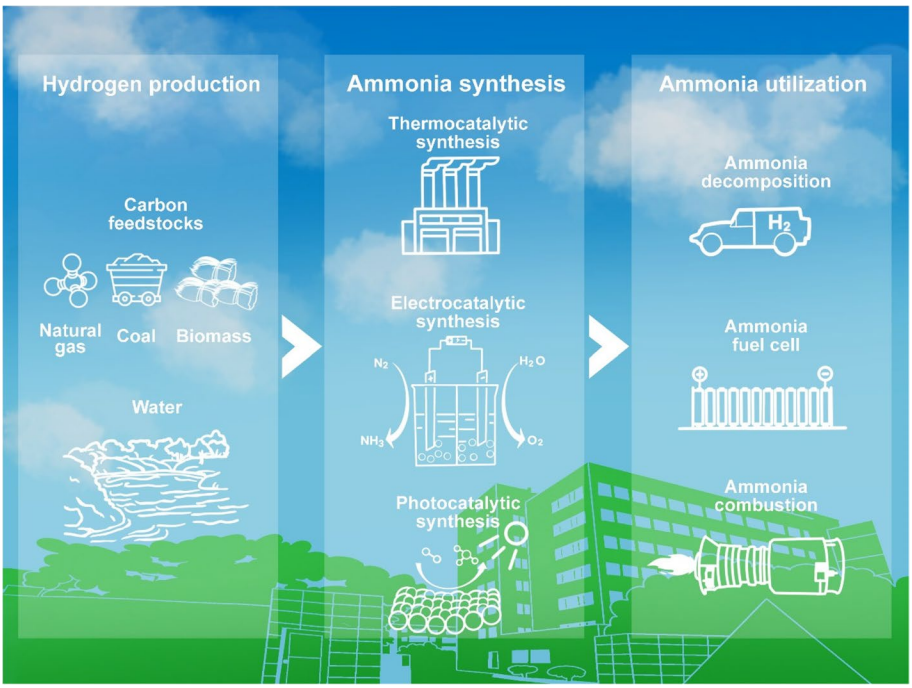


**Fig. 1** The key steps of energy storage and utilization via ammonia. They involve hydrogen production, ammonia synthesis and ammonia utilization

and photocatalytic synthesis (Fig. 1) [16–21]. The HB process for ammonia synthesis is a typical thermocatalytic process. It requires high temperature and high pressure (>400 °C; >10 MPa) [22], to achieve high-efficiency synthesis of ammonia. The electrocatalytic synthesis of ammonia is a mild process. The electricity can be generated by renewable energy [23], such as solar, wind and hydropower. In addition, the photocatalytic synthesis of ammonia directly employs photon energy to implement the catalytic conversion [24]. Its major advantages are mild reaction conditions, low energy consumption and low pollution. Until now, the considerable progress has been made in the three categories of ammonia synthesis. It is valuable to summarize and analyze the catalytic designs and mechanisms in recent years, thereby promoting the development of ammonia synthesis at low cost with low pollution.

Based on artificial synthesis of ammonia, rational utilization of ammonia arouses public concern. Usually, agricultural fertilizers and industrial chemicals are the main ways of ammonia utilization, but it is necessary to explore new approaches for rational utilization of ammonia. In the past few years, ammonia utilization, via ammonia decomposition, ammonia fuel cells and ammonia combustion (Fig. 1), have attracted a great deal of interest [25–27]. The ammonia decomposition can produce hydrogen as a green energy [28]. The ammonia fuel cells are convenient facilities for conversion of ammonia into electric energy [29]. The ammonia combustion will help to decrease consumption of fossil resource, and lower environmental pollution [30]. To rationally utilize ammonia in the near future, it is significant to overview the latest progress and catalytic designs for these emerging fields.

In terms of the energy cost and energy efficiency, the energy storage and utilization via ammonia also possess a high feasibility. At present, the energy cost of hydrogen production from renewable energy is around 4.3 ~ 5.1 kWh/$Nm^3$ $H_2$, and the energy efficiency is about 69% ~ 82%. The ammonia synthesis from $H_2$ and $N_2$ consumes energy for compression, and the energy cost is around 200 ~ 500 kWh/t $NH_3$ with an energy efficiency of around 72% ~ 80%. In addition, there are two possible routes for power generation from ammonia, including: 1) ammonia → pure hydrogen → power, and 2) ammonia → power. The first route possesses an energy efficiency of around 25% ~ 50%. The second route has a different efficiency of about 32% ~ 49%, due to utilization of waste heat for ammonia cracking. Considering the energy recycling, the total energy efficiency of power → ammonia → power process should be in the range of around 20% ~ 40%. We believe that the energy costs and energy efficiencies will attract great interests

to develop energy storage and utilization via ammonia in the future energy system.

Herein, we comprehensively review recent progress and discuss challenges for hydrogen production, ammonia synthesis and ammonia utilization. The important processes and catalytic designs are outlined and discussed, in hydrogen production from carbon feedstocks and water. The catalytic designs and mechanisms are summarized and analyzed, according to ammonia synthesis via thermocatalysis, electrocatalysis and photocatalysis. In addition, the important processes and catalytic designs of ammonia utilization are overviewed, on the bases of ammonia decomposition, ammonia fuel cells and ammonia combustion. We expect that the perspectives of this review can promote development of low-cost and eco-friendly ways for energy storage and utilization via ammonia.

## 2 Hydrogen production

In 2021, the global production of hydrogen was 94 million tons (Mt) [31]. It was mainly produced from fossil fuels (such as 62% from natural gas, 19% from coal, and 18% from by-product of naphtha reforming), while only 35 kilotons of $H_2$ from water electrolysis, shown in Fig. 2. At present, many catalytic processes (e.g., steam reforming (SR), partial oxidation (PO), mixed reforming, autothermal reforming (ATR), tar reforming, dry reforming of methane (DRM), water electrolysis, water photolysis, etc.), have been involved in hydrogen production from carbon feedstocks and/or water [32]. It is proposed that hydrogen production in China will reach up to 130 million tons in 2060, and about 70% of the hydrogen will be produced from water electrolyzers using renewable energy.

### 2.1 Hydrogen production from carbon feedstocks

Hydrocarbon reforming is one of the critical processes for hydrogen production from carbon feedstocks. For which, group VIII metals (such as Ru, Rh, Pt, Ir, Ni, and Co) based catalysts are employed, among which Ni catalyst is the most commonly used in industry, due to its good activity/cost ratio. However, Ni catalyst encounters two major challenges, i.e., carbon formation and sintering of Ni particles. In recent decades, significant progress has been made in the design and preparation of Ni-based reforming catalysts. Many strategies are employed to improve the catalyst performance, for instance, regulating the metal-support interaction, alloying Ni with a second metal, or controlling the Ni particle size, and so on.

Liu et al. [33] found that the $Ni/CeO_2$ is a highly efficient and stable catalyst for DRM at low temperatures (700 K). Methane could dissociate on $Ni/CeO_2$ at temperatures as low as 300 K, generating $CH_x$ and $CO_x$ species on the surface of the catalyst. The strong metal-support interaction (SMSI) activated Ni for the dissociation of methane, and prevented the deposition of carbon

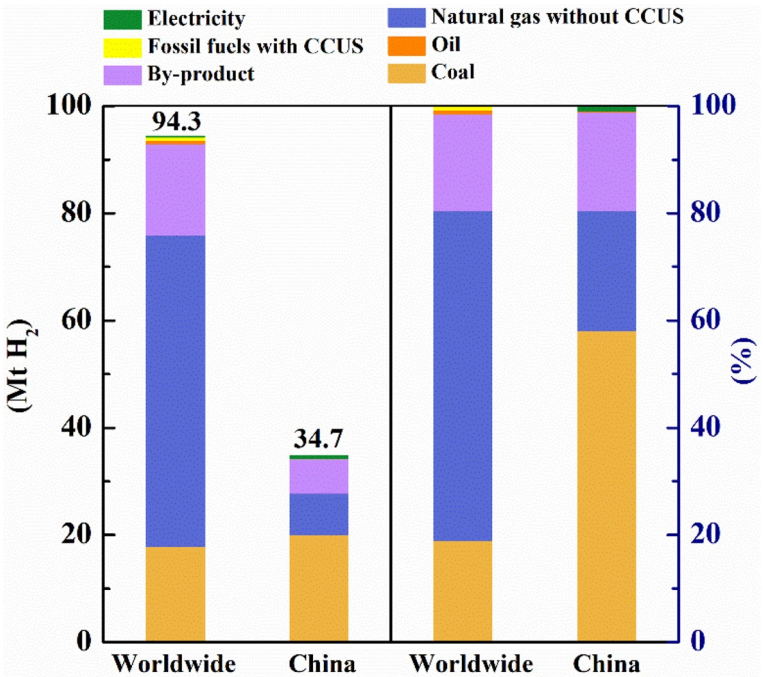


**Fig. 2** Sources of hydrogen production in 2021 in the worldwide and in China

and deactivation. Wang et al. [34] reported that the Ni/$ZrO_2$ was active for DRM at 400, 320, and 300 °C without deactivation during a 10 h reaction, achieving both a stable $CH_4$ TOF of 0.26 $s^{-1}$ and a $CO_2$ TOF of 0.18 $s^{-1}$ at 320 °C. The oxygen vacancy close to the $Ni^0$ site, which would obtain more charge transfer, could promote the adsorption of $CO_2$ and cleavage of the C=O band, forming bidentate carbonate species. These intermediate bidentate carbonate species decomposed to CO and O species to rebuild the interface of Ni–O-Zr as well as the $Ni^0$ site. That is to say, the interface of Ni–O-Zr could promote the removal of carbon, while the oxygen vacancy could promote the activation of $CO_2$ to form an interface and recover the $Ni^0$ species, therefore, enhancing their catalytic stability.

Alloying Ni with a second metal such as Fe, Co, and Cu is an effective way to suppress coke deposition. Ni–Fe alloy catalyst has attracted much attention, due to its significant enhancement of coke resistance. Kim et al. [35] attributed the coke resistance of Ni–Fe alloy to the $Fe^{2+}/Fe^0$ redox cycle in the dry reforming of methane. De-alloying of Ni–Fe occurred when the Fe was partially oxidized to FeO, forming a Ni-richer Ni–Fe alloy; and the FeO could be further reduced by carbon deposits, leading to a reduced coke formation. However, many of the alloy catalysts are inhomogeneous in structure, composition and size, and more efforts are needed to develop uniform alloy catalysts. In this regard, using hydrotalcite-like compounds (HTlcs) as precursors appear to be a good approach, from which several well-dispersed and composition-uniform alloy catalysts, e.g., Ni–Fe [36], Ni-Co [37], and Ni-Cu [38], had been obtained.

Ni particle size is a key parameter for determining coke deposition, and Ni nanoparticles (NPs) with small sizes have high coke resistance. To obtain well-dispersed Ni NPs and inhibit the sintering of Ni NPs, confining Ni NPs with a protective shell or matrix is a promising approach. Various confined catalysts had been developed, for instance, immobilized Ni NPs in channels of mesoporous materials (SBA-15, SBA-16, MCM-41, TUD-1, KIT-6, silicalite-1, MFI zeolite), core–shell Ni@$SiO_2$ [39], yolk-shell Ni@$SiO_2$ [40], $Al_2O_3$-coated Ni/$Al_2O_3$, and $SiO_2$-coated Ni/$SiO_2$. The confined structure supplies a powerful way to prevent metal sintering at high temperature, because the metal particles can be completely separated. However, mass transfer may be hindered by the shell structure to some extent, which should be considered in the design and preparation of catalysts with confined structures.

Additionally, Liang et al. [41] prepared an MFI zeolite encapsulated Ni-Co alloy catalyst using a one-pot method. The 10Ni1Co@ADM-0.1 catalyst showed $CH_4$ conversion of 71% and $CO_2$ conversion of 93% at 700 °C, with a little loss of activity during 100 h of DRM reaction. The formation of Ni-Co alloy favored the electron transfer from Co to Ni, which led to electron-rich Ni sites that enhanced the breaking ability of the C-H bond. On the other hand, the encapsulated structure efficiently promoted the close contact of metal and support. The $CH_x$* species, formed on metallic sites, could rapidly react with $CO_2$ adsorbed on MIF zeolite. Furthermore, the oxygen vacancies on the catalyst surface could adsorb $CO_2$ and generate active adsorbed oxygen species, to remove the C* species from methane complete dehydrogenation.

Ni single-atom catalysts (SACs) are demonstrated to be highly coke-resistant. Akri et al. [42] developed a $Ni_1$/HAP-Ce SACs catalyst, where the Ni was deposited on the Ce-substituted hydroxyapatite by strong electrostatic adsorption (Fig. 3a). The $2Ni_1$/HAP-Ce catalyst showed high activity and stability in DRM at 750 °C for 100 h (Fig. 3b), with negligible carbon deposition. The Ce doping of HAP induced a strong metal-support interaction, which stabilized the Ni singe atoms against sintering. DFT calculation suggests that the ceria-bound isolated Ni atoms were highly active for cleavage of the first C-H bond, while the $CH_3$ dissociation was thermodynamically unfavorable (Fig. 3c). Subsequently, the resulting $CH_3$ species are oxidized to $CH_3O$, followed by $CH_3O$ dehydrogenation to $CH_2O$, CHO, and CO without carbon deposition (Fig. 3d). It was concluded that the Ni single atoms were intrinsically coke-resistant, due to their unique ability to merely activate the first C-H bond in $CH_4$ and avoid deep decomposition of methane into carbon. These findings highlight that Ni SACs can be a promising coke-resistant catalyst.

As a renewable carbon resource, bio-ethanol has attracted much attention, to produce hydrogen through ethanol steam reforming (ESR). Meng et al. [43] reported a RhNi/$TiO_2$ (0.5 wt.%Rh) catalyst, with well-defined strong bimetal-support interaction. It afforded exceptional $H_2$ yield (61.7%) and catalytic stability (300 h) at the temperature as low as 400 °C. The RhNi bimetallic nanoparticle, with a reversible $TiO_2$ coating, exhibited a multiple electron transfer pathway at the interfacial active sites (Rh-$Ni^{\delta-}$-$O_v$-$Ti^{3+}$). The geometric and electronic structure of interfacial active sites reduced the binding ability of species with $COO^-$ structure ($CO_2$, carbonate, or formate). This facilitated the generation and transformation of formate intermediate from reforming processes of CO/$CH_x$, which ensured a prominent hydrogen production rate and catalytic stability.

Gasification is another key technology for clean utilization of solid fuels (such as coal, biomass, petroleum residues, and municipal solid wastes (MSW)). The solid carbon feedstocks can be gasified at high temperatures (> 800 °C) in the presence of steam and/or oxygen,

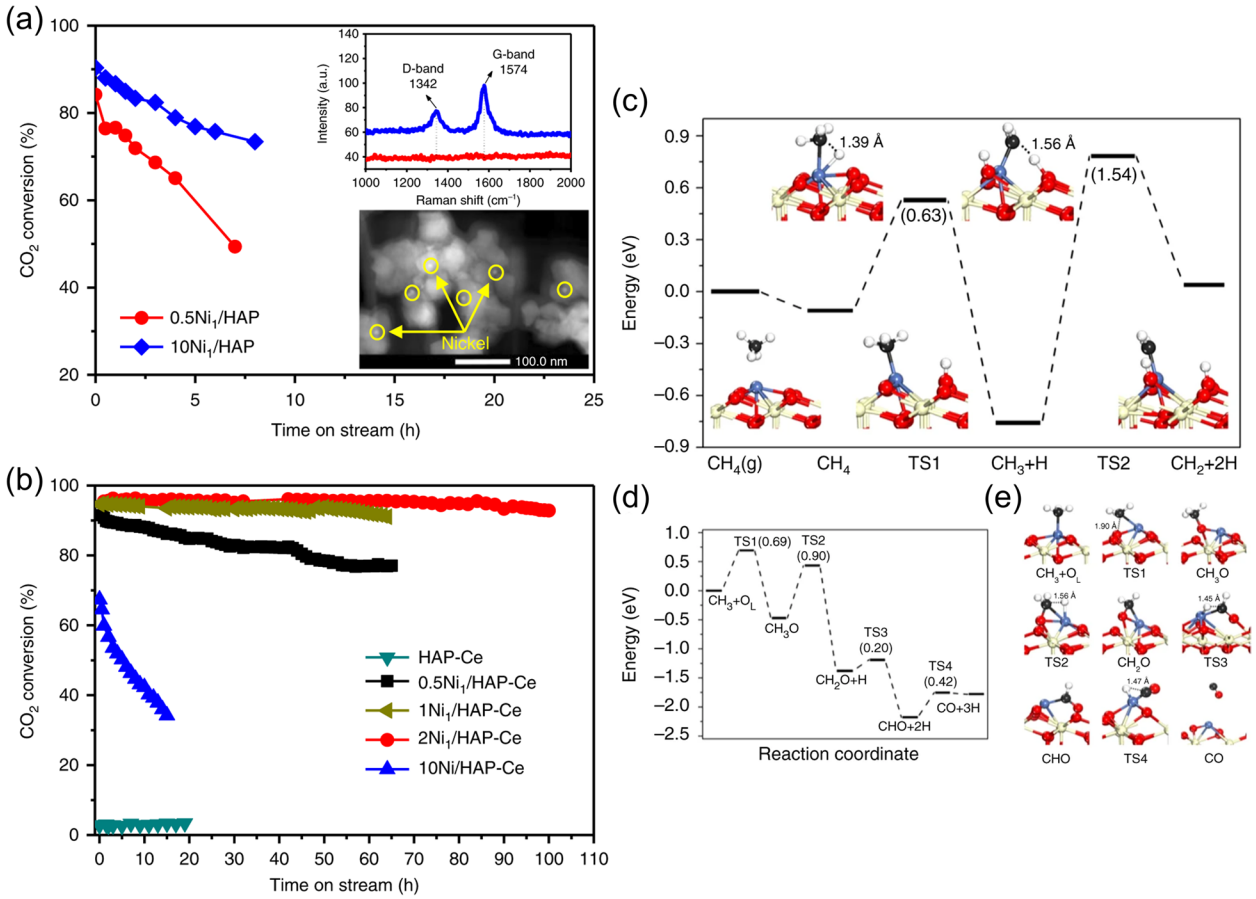


**Fig. 3** DRM performance over (**a**) Ni/HAP and (**b**) Ni/HAP-Ce catalysts. Conditions: T = 750 °C, CH4/CO2/He = 10/10/30, GHSV = 60,000 mL h−1 gcat−1, inset is Raman spectra of spent 0.5Ni1/HAP and 10Ni/HAP after reaction at 750 °C and STEM image of 0.5Ni1/HAP after 7 h reaction. DFT calculation of CH4 decomposition: (**c**) potential energy diagram from DFT calculations of CH4 dissociation over Ni1/CeO2, (**d**) potential energy diagram from DFT calculations of CH3 oxidation and CH3O dehydrogenation, and (**e**) corresponding geometries over Ni1/CeO2. Numbers in parathesis indicate the activation barriers for elementary steps in eV. Optimized structures for reaction intermediates are shown inset (Ce: yellow, Ni: blue, O: red, C: black, H: white). Reproduced with permission from ref. 42. Copyright (2019) Nature Publishing Group

producing a gaseous mixture of $H_2$, $CO_x$, $CH_4$, light hydrocarbons, together with tar, char, ash, and other trace contaminants ($NH_3$, $H_2S$, HCN, HCl). Particularly, tar is problematic, which can cause several problems such as condensation in exit on downstream equipment, resulting in serious operational interruptions. Hence, catalytic reforming of tar has received great interest in research [44].

Tar, which contains single-ring to 5-ring aromatics (e.g., benzene, toluene, phenol, naphthalene), has a high potential for carbon deposition. Therefore, the development of a cost-effective and efficient catalyst for tar reforming remains challenging. Lin et al. [45] reported a Ni/$Ce_{0.8}Zr_{0.2}O_2$ nanorod catalyst for steam reforming of toluene, which attained 99.5% toluene conversion at 600 °C and GHSV of 24,000 $h^{-1}$. The catalyst showed much higher catalytic activity and coking resistance than other Ni-based catalysts. The good catalytic performance was ascribed to the SMSI between Ni and the predominant exposed facet of $Ce_{0.8}Zr_{0.2}O_2$. The SMSI made the Ni atoms to stably anchor to the oxygen vacancies, and induced the electron transfer among them (from $Ce^{3+}$ and $Zr^{\delta+}$ to $Ni^0$ and then to $O^{2-}$), keeping Ni in the reduced state. Besides, the SMSI facilitated the conductivity of electrons/holes of $Ce^{3+}$ that improved the dissociation activity of $H_2O$ as well as the activation of lattice oxygen. As a result, the C–H activation, $H_2O$ dissociation, and the formation and transportation of active oxygen species were enhanced, which was conducive to toluene reforming as well as coking resistance. However, to some extent, the catalyst was deactivated during 10 h reaction, which was attributed to the covering of Ni active sites by amorphous carbon. So far, the most of the reported catalysts are still not stable for long-time operation. Therefore, exploration of a cost-effective and efficient catalyst for

tar reforming remains significant for coal or biomass gasification.

### 2.2 Hydrogen production from water

Extracting hydrogen from water, using renewable energy, is found to be a promising route, which is a green way with zero emissions. The future hydrogen will be generated by water splitting, which may account for 70% in 2060. There are many ways, such as electric, photonic, heat, and a combination of those techniques. Among them, water electrolysis via electric energy, which combines the hydrogen evolution electrode reaction (HER) and oxygen evolution electrode reaction (OER), has been widely researched [46]. The three main types of water electrolyzers are shown in Fig. 4, i.e., Alkaline (ALK) and Pronton Exchange Membrane (PEM) water electrolyzer, and Solid Oxide Electrolysis Cell (SOEC).

Pt-based catalysts are found to be efficient for HER. However, due to the scarcity of Pt, many efforts have been put on improving the catalytic performance with low Pt loading. The PtRu alloy embedded in porous carbon spheres was fabricated [47], which showed equivalent activity to the commercial one, while the Pt loading was low to 0.2%. The Pt supported on N-doped graphene nanosheets was prepared through atomic layer deposition [48], which showed excellent activity and stability, owing to the presence of Pt single-atom of clusters. Non-noble metal catalysts, such as metal sulfide and metal phosphide catalysts, are also active for HER. Transition metals, such as Fe, Co, Ni, Cu, Mo and W, have been found to be competitive candidates.

For example, $MoS_2$ ultrathin nanosheets with abundant edge active sites, which is generated from the controllable production of induced defects, can show excellent activity for HER [49]. Micro- and nano- $CoS_2$ catalysts were fabricated in three microstructures, and the $CoS_2$ nanowires show the best electrocatalytic performance, prosperous stability, cycle performance and hydrogen production rate. It was attributed to its high surface area and effective release of surface bubble [50]. On the metal phosphide catalysts, $Ni_{12}P_5$ single crystal, prepared by water-in-oil microemulsion method, was high in specific surface area (222.5 $m^2\ g^{-1}$) with hollow sphere morphology [51]. It thus had a large number of active sites and high structure stability, showing excellent catalytic activity and stability in acidic HER. Multi-faceted CoP nanoparticle was prepared by the reaction of nanoparticle and trioctylphosphine, and supported on Ti plate [52]. It was reported that the prepared CoP possessed high activity and high stability under strongly acidic conditions.

OER is found to be the rate determining step in water electrolysis, because electron transfer is involved in OER, which is slow in dynamics. The Ir- and Ru-based catalysts were reported to be promising catalysts for OER. The $Ce_{0.2}$-$IrO_2$@NPC, prepared by supporting Ce doped $IrO_2$ on nanoparticle porous carbon, showed a low

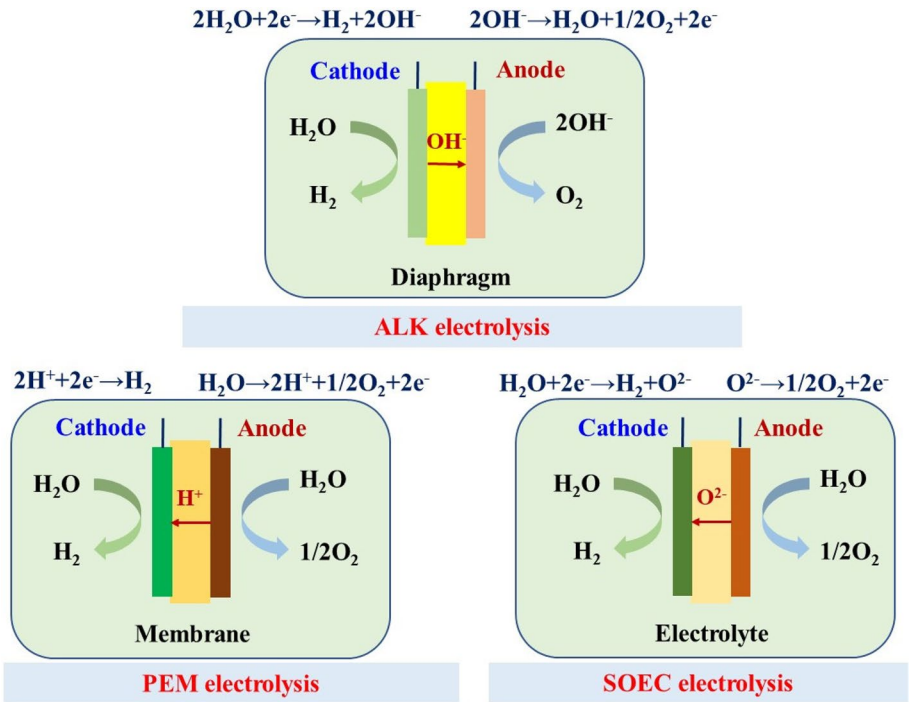


**Fig. 4** Schematic presentation of the three main types of water electrolyzers

overpotential of 224 mV and excellent stability of 100 h in 0.5 M $H_2SO_4$ at 10 mA $cm^{-2}$. This should be attribute to the modification of its electronic structure [53]. The Ru nanoparticles with rich grain boundaries, fabricated by the laser ablation, exhibited a low overpotential of 202 mV. It is lower than that of commercial $RuO_2$ (305 mV) [54]. However, the applications of Ir- and Ru-based catalysts are limited due to the low abundance, high cost and instability. Therefore, many efforts on non-noble metal OER catalysts have triggered considerable interests.

First, adjusting the electronic structure of the OER electrocatalyst by additive doping: for instance, the cobalt–nickel bimetallic oxides, supported on boron-doped graphene, was prepared with a Co/Ni ratio of 1:1 [55]. It had a good OER electrocatalytic performance under alkaline conditions, owing to the regulation of charge distribution in bimetallic oxides and strong synergistic coupling effect. Second, improving the mass transfer on the electrode by constructing unique catalyst structures: for example, the $MoO_3$/Ni-NiO with amorphous NiO nanosheets was prepared by a two-step electron-deposition method, which possessed two heterojunctions of Ni-NiO and $MoO_3$-NiO [56]. The two heterojunctions reduced the energy barrier and synergistically affected the OER efficiency, showing excellent electrochemical performance. Third, regulating the coordination of local environment by introducing anion and/or cation: for example, the carbonyl sulfide with a unique electronic structure was synthesized by an anionic regulation strategy [57]. The electrochemical anionic regulation process enabled the accurate substitution of sulfur anions, thus regulating the electronic structure and improving the electrochemical activity.

Photonic energy can also be employed to produce hydrogen from water via photocatalytic process, but it is low in efficiency. As shown in Fig. 5 [58], there are three key steps in photocatalytic production of hydrogen: light absorption, charge separation and surface reaction. When the bottom of the conduction band of a catalyst is more negative than the potential of $H^+/H_2$, and the top of the valence band is more positive to the potential of $O_2/H_2O$, the photocatalysis of water would thermodynamically occurs.

To date, catalysts for photocatalysis of water are reported to be metal oxides, metal sulfides, $C_3N_4$ and so on. Metal oxides that have flexible electronic structures, can effectively catalyze the photolysis of water. The 18-facet STO with anisotropy was prepared and supported with Pt-$Co_3O_4$ by Mu et al. [59]. Its photocatalytic performance was 5 times higher than that of a hexagonal STO catalyst, and its quantum efficiency was 4 times higher. Sun et al. [60] took the advantage of quantum confinement effect, to prepare quantum sized $BiVO_4$. It showed high activity for water splitting, attributed to the negative shift of the conduction band of $BiVO_4$. The Au@$TiO_2$, prepared by dispersing Au on hollow mesoporous $TiO_2$, displayed a hydrogen evolution rate of 1600 μmol $g^{-1}$, due to a better separation of photogenerated charges [61]. Metal sulfide is another typical photocatalyst that can utilize visible light from solar. For instance, the Cu/ZnS microspheres, fabricated by microwave irradiation method, showed a hydrogen evolution rate of 973.1 μmol $h^{-1}$ $g^{-1}$ and good stability for 48 h test,

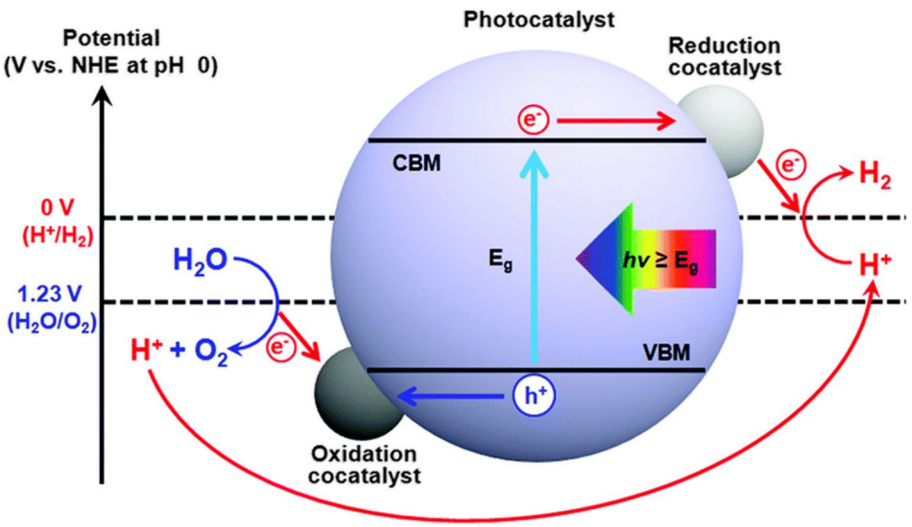


**Fig. 5** Schematic diagram of photocatalytic hydrogen production mechanism. Reproduced with permission from ref. 58. Copyright (2019) royal cociety of chemistry

when the doping amount of Cu was 2 mol% [62]. In addition, carbon nitride has a lower band gap (2.7 eV), and higher valence and conduction band positions. When embedding carbon nanodots into the $C_3N_4$ matrix [63], the solar energy conversion efficiency can reach up to 2%, and excellent stability is performed.

Photo-electric coupling (PEC) production of hydrogen from water has also been extensively researched, which introduces extra energy to the photocatalytic system and promotes the separation of electron holes. The conversion efficiency of PEC on an anode semiconductor depends on the light absorption, charge separation-transfer and charge utilization [64]. Narrow band gap semiconductors, such as $BiVO_4$, $Ta_3N_5$, etc., can extend the spectral absorption range to the visible region [65, 66]; while wide band gap semiconductors, such as $TiO_2$, ZnO, etc., can improve the light trapping ability [67, 68]. Morphological control, metal/nonmetal doping and surface reconstruction, can accelerate the separation and transportation of photogenerated charges [69–71].

In the photoelectrical splitting of water, researchers are committed to developing OER catalysts, which have good compatibility with anode semiconductors and can effectively improve the charge efficiency [72]. Ultrathin β-FeOOH catalysts with rich oxygen vacancies were deposited on the nano-porous $BiVO_4$ electrode by Zhang et al. [73]. The catalyst showed a photocurrent of 4.3 mA $cm^{-2}$ at 1.23 $V_{RHE}$, which was 4 times higher than that of the $BiVO_4$ electrode and about 2 times higher than that of the β-FeOOH catalyst. The Ni-doped FeOOH, coated on different anodes, showed a high charge transfer efficiency, when the one-step hydrothermal method was employed [74]. Coating with $WO_3/BiVO_4$, it achieved a current density of 4.5 mA $cm^{-2}$ and a charge transfer efficiency of 91% at 1.23 $V_{RHE}$. Additionally, a two-dimensional grid was fabricated by the connection of phenol ligands and metal ions, and a uniform thin film assembly layer on porous Mo-doped $BiVO_4$ was prepared [75]. Compared with the traditional OER catalyst island on the anode surface, the coating of the thin film reduced the photo-corrosion and improved the stability. Further, Kim et al. [76] used two different OEC catalyst layers to prepare $BiVO_4$/FeOOH/NiOOH composite electrode, and the photocurrent density of the electrode reached 2.73 mA $cm^{-2}$ at 0.6 $V_{RHE}$. Among them, the $BiVO_4$/FeOOH junction can effectively reduce interfacial recombination, while NiOOH produces Helmholtz layer potential drop between OER catalyst and electrolyte.

Hydrogen production from fossil fuels accounts for the major hydrogen demand (> 99%) nowadays, because of price advantage. For instance, in China, the price for $H_2$ from coal and natural gas is 9.3–15.3 and 19.5–33.1 CNY/kg, respectively. Although the prices are relatively low, they generate high $CO_2$ emissions (e.g., 20 kg $CO_2$ / kg $H_2$ from coal; 9.5 kg $CO_2$/kg $H_2$ from natural gas), and low efficiencies of energy conversion (e.g., 53.6% from coal; 55.8% from natural gas). In contrast, the price of $H_2$ from water electrolysis is quite dependent on electricity price, and the cost of electricity accounts for 87% of the hydrogen. But its efficiency of energy conversion can reach 72.7% via water electrolysis. Therefore, the amount of hydrogen production from water with zero-emission has been increasing dramatically in recent years, aiming to meet the goal of carbon neutrality. For which, various catalysts with unique structures, such as core–shell, metal alloy and complex metal oxides, have been fabricated to achieve high catalytic activity and stability.

## 3 Ammonia synthesis

Ammonia is a fundamental building block in the chemical industry, and also a promising hydrogen energy carrier [5, 77, 78]. According to the statistics, the output of ammonia is around 180 million tons in 2021, and 80% of the produced ammonia is used as fertilizer in agriculture [79]. The ammonia synthesis industry is closely related to the survival and development of human beings, which is of great significance in the history of the chemical industry. Ammonia synthesis is a model of the successful application of basic theory in industry, and also creates high-pressure technologies in the chemical industry. Since the first ammonia synthesis device started to produce ammonia in 1913, the ammonia synthesis industry has made great progress [80]. Nowadays, different catalytic methods of ammonia synthesis have been developed, mainly including thermocatalytic synthesis, electrocatalytic synthesis, and photocatalytic synthesis. The characteristics, challenges, and development of different methods for ammonia synthesis are reviewed and discussed as shown below.

### 3.1 Ammonia synthesis via thermocatalysis

Large-scale ammonia synthesis ($N_2 + 3H_2 \rightarrow 2NH_3$) is based on the thermocatalytic pathway via Haber – Bosch (HB) process, which requires harsh reaction conditions (400–500 °C, 10–30 MPa) [81, 82]. The $H_2$ feed gas is commonly produced from fossil fuels via the route of "steam cracking → water gas shift reaction → desulfurization and decarbonization → $H_2$ purification". Then the highly purified $H_2$ reacts with $N_2$ of air separation, to generate $NH_3$. The whole process of ammonia synthesis consumes around 1 ~ 2% of global energy, and results in 1.5 ~ 1.9 tons of carbon dioxide ($CO_2$) emissions per ton of ammonia [83, 84]. In recent years, the renewable energy-driven HB process via the route of "renewable energy power → electrolytic $H_2$ production → $NH_3$ synthesis → $NH_3$ utilization" has aroused great attention (see

in Fig. 6), due to energy-saving and environment-friendliness for ammonia synthesis [85, 86]. The integration of ammonia synthesis and electrolytic water would facilitate the miniaturization of ammonia synthesis, to enable local scale, distributed energy storage. However, via water electrolysis, the output pressure and temperature of $H_2$ are usually less than 5 MPa and 400 °C, respectively. They are unmatched with the conditions used for industrial ammonia synthesis. To avoid the use of expensive pressure-elevated facilities, it is pivotal to develop efficient catalysts for ammonia synthesis under mild conditions.

Ammonia synthesis under mild conditions confronts the challenge of low ammonia productivity, due to the steady $N_2$ molecules and the scale relation (inverse relationship of the dissociation barrier of $N_2$ and the desorption energy of $NH_x$ ($x=1\sim3$) species on transition metals) [87, 88]. To increase ammonia synthesis rate at mild conditions, many strategies have been taken to promote $N_2$ activation and/or circumvent the scale relation. The optimization of promoters over the catalysts is essential to promote $N_2$ activation and ammonia synthesis [89, 90]. The alkali metals, alkaline-earth metals, and rare-earth metals have been developed as efficient promoters for ammonia synthesis. To enhance $NH_3$ synthesis performance, it is important to identify the contributing ingredient of promoters, and enhance the interaction between promoter and active centres. For instance, it was reported that in situ dosing of Cs metal vapor into Ru-based catalysts showed an order of magnitude higher activity for $NH_3$ synthesis, compared to the ones prepared by traditional method. This was attributed to the remarkable promotional effect of Cs metal than Cs-O and Cs-OH species on ammonia synthesis [91].

The development of advanced supports for catalysts is necessary to enhance ammonia synthesis performance. The properties of supports have a significant impact on particle size, morphologies, as well as electronic structure of the supported metals. Recently, inorganic electrides such as C12A7:e−, $Y_5Si_3$:e−, and LaCoSi, with a low function work, were reported to exhibit a strong electron-donation ability, to promote $N_2$ cleavage over Ru or Co active sites (Fig. 7a) [92–94]. In addition to the inorganic electrides, rare-earth oxides (such as $CeO_2$, $SmO_2$, $BaCeO_3$ and $La_{0.5}Ce_{0.5}O_{1.75}$) also exhibit strong electron-donation ability after reduction treatment, because of the formation of abundant oxygen vacancies. Hence, the rare-earth oxides with transition metal centers show remarkable performance of ammonia synthesis at mild conditions (Fig. 7c) [95–98].

The construction of dual active sites is an efficient strategy, to circumvent scale relation and realize high-efficiency ammonia synthesis. For instance, Chen et al. reported that the catalysts of LiH mediated transition metal can break scaling relations, to achieve low-temperature ammonia synthesis, through the LiH-mediated nitrogen transfer and hydrogenation from transition metal sites [88]. Other hydrides (such as KH, NaH, $CaH_2$, and $BaH_2$) also exhibit the similar role as LiH, to promote $NH_3$ synthesis (Fig. 7b) [99]. Another typical dual-site system is the transition metal/nitrides catalysts (Fig. 7c), which can efficiently catalyze $NH_3$ synthesis, due to the separated sites for $H_2$ adsorption over TMs and facile $N_2$ activation over nitride ion vacancies [100, 101]. It was reported that the nitrides with low formation energy of nitrogen vacancy ($E_{NV}$) are beneficial to promote $N_2$ activation and $NH_3$ synthesis at mild conditions.

The regulation of particle size of active metal has a significant effect on ammonia synthesis performance. Ammonia synthesis is a structure-sensitive reaction, where a minute variation of catalyst structure would lead

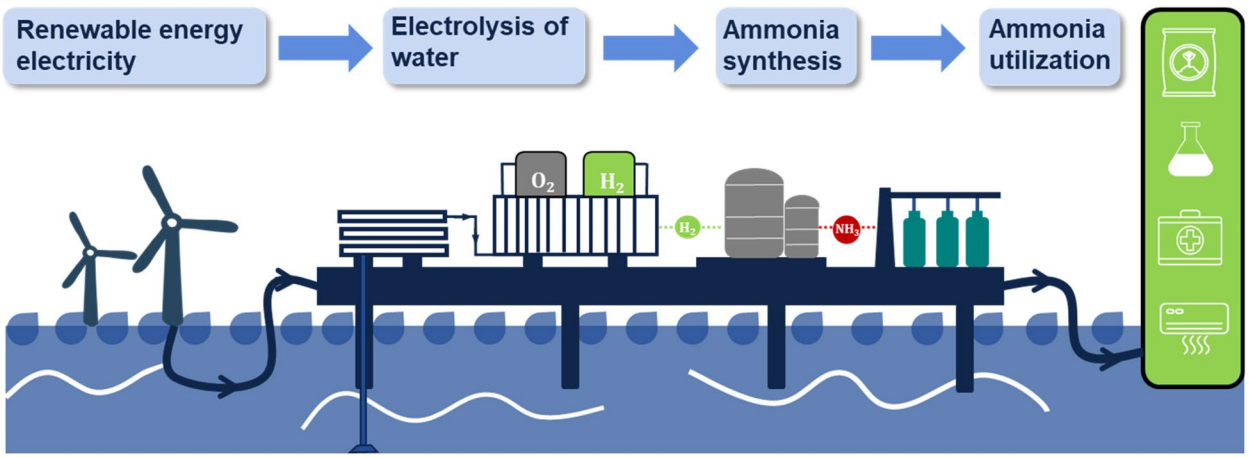


**Fig. 6** Schematic diagram of renewable energy-driven HB process

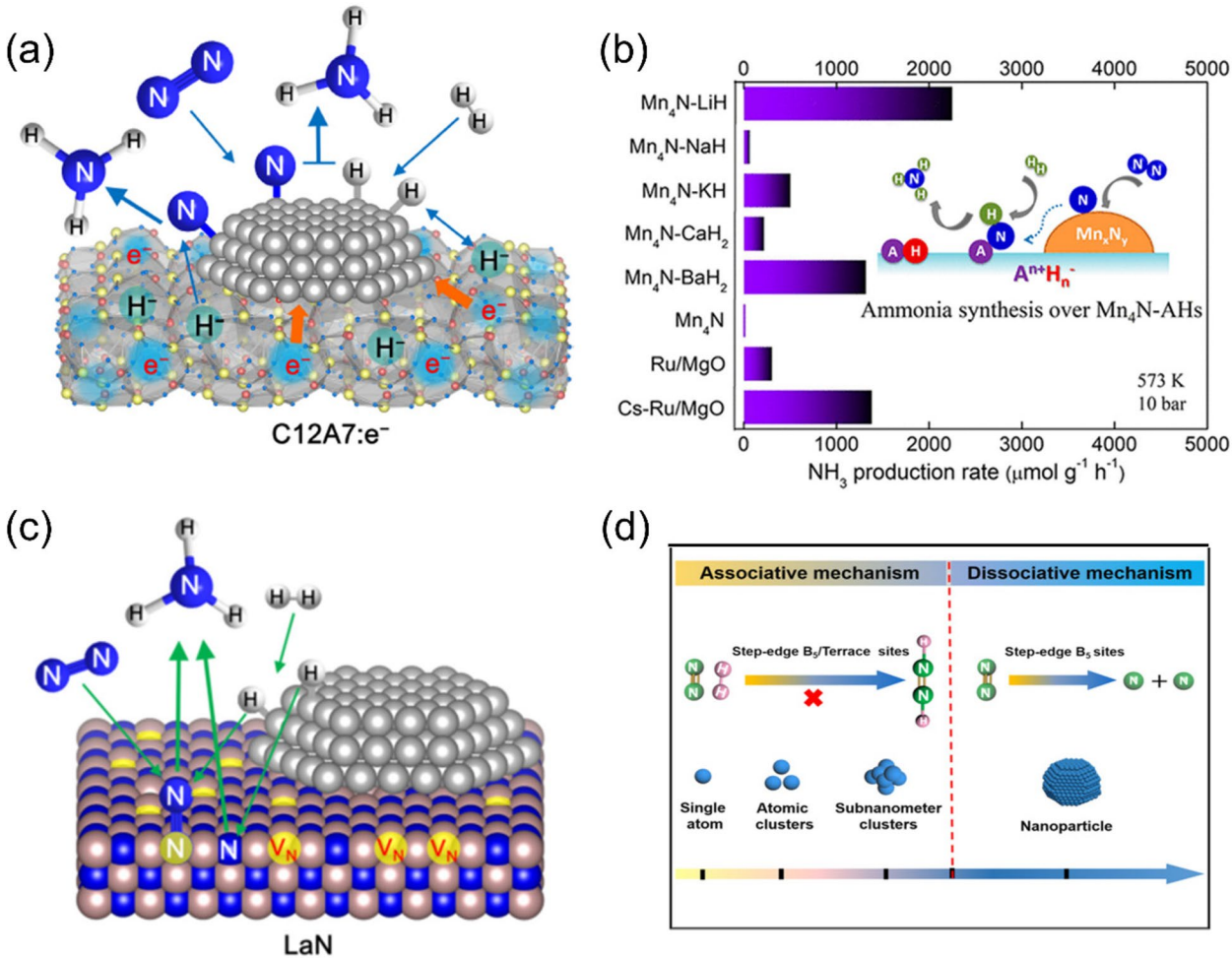


**Fig. 7** **a** Reaction mechanism for ammonia synthesis over TM-loaded C12A7:e – . Reproduced with permission from ref. 92. Copyright (2012) Nature Publishing Group. b The ammonia synthesis rates on hydride-mediated Mn4N catalysts. Reproduced with permission from ref. 99. Copyright (2017) Nature Publishing Group. c The possible mechanism of ammonia synthesis over Ni/LaN. Reproduced with permission from ref. 100. Copyright (2020) Nature Publishing Group. d Ammonia synthesis pathway over Ru catalysts with different sizes. Reproduced with permission from ref. 103. Copyright (2022) Elsevier

to a dramatic change of activity. In terms of Ru-based catalysts, it is recognized that the most active sites for $N_2$ dissociation are ensembles of five Ru atoms (the so-called B5 sites) over Ru nanoparticles [102]. Recently, it was reported that the reaction mechanism of ammonia synthesis shifts from dissociative mechanism to associative mechanism, when the particle size of Ru decreases from nanoparticles to subnanometric clusters and single atoms (Fig. 7d) [103]. The Ru single atoms and atomic clusters without the presence of B5 sites can trigger direct hydrogenation of $N_2$ via an associative route for $NH_3$ synthesis. The outstanding ammonia synthesis performance can be realized over Ru atomic cluster catalyst. It provides an important implication to design efficient catalysts of ammonia synthesis via the modulation of particle size.

Thermocatalytic ammonia synthesis, under relative low temperatures and pressures, can not only lower the quality standard of production equipment, but also reduce energy consumption and $CO_2$ emissions. It is meaningful for the magnificent blueprint of carbon-neutrality. The exploitation of advanced catalysts is crucial to promote the application of ammonia synthesis under mild conditions. The optimizations of promoters, supports, and active centres of catalysts are efficient strategies to improve the catalytic performance of ammonia synthesis rate. The regulation of reaction mechanism also provides a possibility to enhance ammonia synthesis rate. In comparison with the direct dissociation of strong N≡N triple bond, the stepwise breaking of N≡N bond via an associative mechanism requires much lower activation energy,

and is easier to occur. Thus, the design of catalysts that can follow associative route for ammonia synthesis, is promising to exhibit high ammonia synthesis rate at mild conditions, analogous to biological nitrogen fixation at ambient conditions.

It is worth mentioning that some researchers have started employing plasma-driven catalysis to carry out ammonia synthesis under mild conditions [104–107]. In the plasma-catalytic ammonia synthesis, the highly energetic electrons, generated by high voltage discharge process, can react with $N_2$ and $H_2$ reactants, to form reactive species (e.g., radicals, excited atoms, molecules, and ions). They can significantly enhance reaction kinetics, and enable thermodynamically unfavorable reactions to proceed under ambient conditions. Notably, with the assistance of plasma, the $N_2$ molecules can be activated to the plasma state, thus lowering the barrier of $N_2$ dissociation. On the basis, the scale relation of ammonia synthesis can be circumvented, and more materials can be served as potential catalysts to realize efficient plasma-catalytic ammonia synthesis.

### 3.2 Ammonia synthesis via electrocatalysis

Electrochemical ammonia synthesis involves the reaction of nitrogen and water via electric energy, to produce ammonia ($N_2 + 3H_2O = 2NH_3 + 3/2O_2$) [23]. The electric power can be generated from renewable solar, wind, and tide energy. The reaction process is clean and pollution-free. It can skip the hydrogen production section of electrolytic water, and has higher theoretical energy efficiency. Thus, it is considered to be one of the most promising technologies for green ammonia synthesis under mild conditions. At present, electrocatalytic ammonia synthesis is difficult to be industrialized, due to the low ammonia synthesis rate and Faraday efficiency. There are three main problems: (1) The stable N≡N triple bond with a high bond energy of 945 kJ $mol^{-1}$ and low proton affinity make $N_2$ difficult to be adsorbed and activated thermodynamically. (2) The solubility of $N_2$ molecules in aqueous electrolyte is as low as ~ 0.61 mM (25 °C, 1 atm), which limits the amount of $N_2$ involved in the reaction. (3) In view of the similar theoretical overpotential required for electrochemical nitrogen reduction reaction (NRR) and hydrogen evolution reaction (HER), the competition of HER is serious in electrochemical ammonia synthesis [4].

According to the above problems, some effective strategies have been proposed in terms of optimization of the catalysts. A series of new metal-based electrocatalysts (such as single-atom catalysts, precious metals and alloys (Au, PtAu, etc.), metal oxides ($Fe_2O_3$, $Co_3O_4$, etc.), metal nitrides, metal sulfides) have been developed for improving the adsorption and activation ability of $N_2$. For instance, Li et al. synthesized a single-atom gold catalyst ($Au_1/C_3N_4$) for electrocatalytic ammonia synthesis [108]. The Faraday efficiency can reach 11.1% (Fig. 8a), outperforming the most of reported catalysts under comparable conditions. Jiang et al. proposed the Mo and phosphotungstic acid (PTA) embedded in multi-walled carbon nanotube catalyst, to enhance the adsorption and activation of $N_2$ [109]. This catalyst presented a high ammonia yield rate of 51 ± 1 μg $mg_{cat}^{-1}$ $h^{-1}$ and an excellent Faradaic efficiency of 83 ± 1% under ambient conditions.

In recent years, the non-metallic electrocatalysts, such as defective carbon materials, boron-based compounds, polycarbon nitride and black phosphorus, have also been developed for enhancement of $N_2$ activation and ammonia synthesis. For example, Wang et al. used a defective black phosphorene to construct a non-precious metal catalyst for efficient electrocatalytic ammonia synthesis

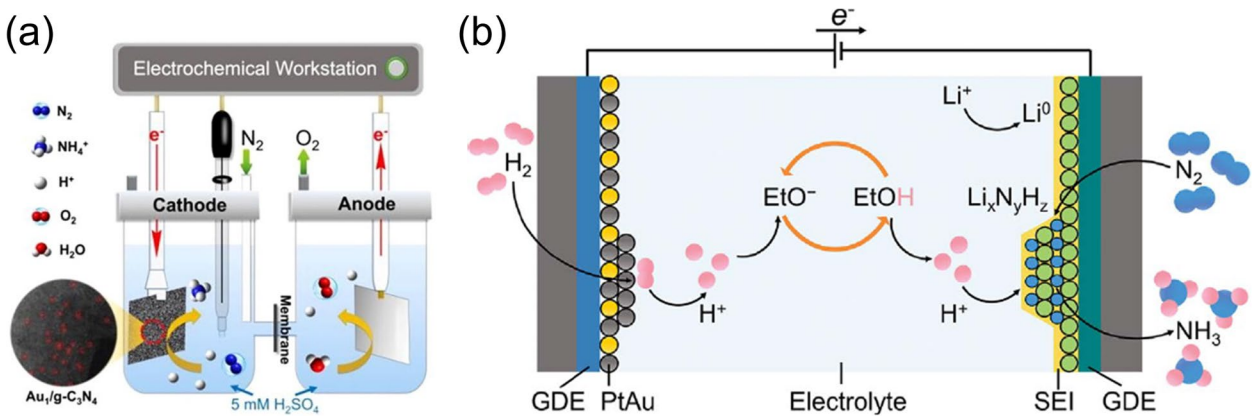


**Fig. 8** **a** An atomically dispersed Au1 catalyst for electrocatalytic ammonia synthesis. Reproduced with permission ref. 108. Copyright (2018) Elsevier. **b** Schematic process of the Li-NRR in a continuous-flow electrolyzer. Reproduced with permission ref. 112. Copyright (2023) Nature Publishing Group

under mild conditions [110]. The ammonia production rate can reach 31.37 ug $mg_{cat}^{-1}$ $h^{-1}$ over the fluorine-stabilized defective black phosphorene.

The optimization of reaction system (such as increasing nitrogen pressure, introducing non-aqueous electrolyte, designing gas diffusion layer, and constructing membrane reaction pool) can improve the concentration of $N_2$ solubility. For example, MacFarlane's team obtained an electrochemical ammonia synthesis rate of 53 nmol $s^{-1}$ $cm^{-2}$ at a Faraday efficiency of 69%, by using inorganic phosphorus as a proton shuttle medium [111]. The introduction of phosphonium salt in this system can avoid the use of sacrificial sources of protons, and also provides additional ionic conductivity, enabling high ammonia production rate.

In addition, based on the feature that lithium metal can react with nitrogen at room temperature, a non-water Li mediated reaction system was designed to transform direct catalytic synthesis into indirect catalytic process ($Li^+ \rightarrow Li_0 + N_2 + H^+ \rightarrow Li_xN_yH_z \rightarrow Li^+ + NH_3$). Nørskov and Chorkendorff et al. used a nonaqueous Li mediated platinum-gold alloy system in a continuous-flow electrolyzer, to achieve low-temperature electrochemical synthesis of ammonia, with a Faraday efficiency of 61% and an energy efficiency of 13.1% (Fig. 8b) [112]. It showed that the classical platinum catalyst is not stable for hydrogen oxidation in the organic electrolyte, but platinum-gold alloy lowers anode potential and avoids decremental decomposition of organic electrolyte.

Besides, particular caution should be taken to exclude the ambient ammonia contamination during electrocatalytic ammonia synthesis, which may be from atmospheric ammonia, equipment, catalytic materials, chemicals and gases. Therefore, stringent experimental protocols have been proposed for electrocatalytic ammonia synthesis, to avoid misinterpretation of results [23]. Moreover, it is better to employ advanced detection methods (such as $^{15}N_2$ isotope labeling and nuclear magnetic resonance spectroscopy) to confirm the actual reduction of $N_2$ in the electrocatalytic system.

The use of renewable energy to achieve electrochemical ammonia synthesis is a hot research topic, but it is difficult to achieve industrialization of electrocatalytic ammonia synthesis at this stage. The development of efficient catalysts and new reaction systems are both essential to increase the yield of ammonia production. Although many efforts have been made, it is still a great challenge to design an electrochemical system with both high catalytic activity and high selectivity. To accelerate the development in this area, future research needs to focus rational design of the electrocatalysts with assistance of artificial intelligence. In addition to the design and development of efficient catalysts, energy cost is also an important point that cannot be ignored. More attention should be paid to reduce the energy consumption of electrochemical ammonia synthesis.

### 3.3 Ammonia synthesis via photocatalysis

Photocatalytic ammonia synthesis is a process of converting $N_2$ and water to $NH_3$ via photonic energy ($2N_2 + 6H_2O \rightarrow 4NH_3 + 3O_2$) [20, 113]. In photocatalytic process, the material is irradiated by sunlight (*hv*), and then the photogenerated electrons and holes ($H^+$) are separated. On this basis, the holes can oxidize water to form $H^+$ and $O_2$, and the electrons can reduce $N_2$ with the assistance of $H^+$ to form $NH_3$. Since solar energy is clean and abundant, photocatalytic ammonia synthesis can convert solar energy into chemical energy for storage. The whole process does not emit carbon dioxide, so it is a green and sustainable pathway for ammonia synthesis. However, at present, the utilization rate of solar energy and the yield of photocatalytic ammonia synthesis are extremely low, which is far away from large-scale application. The main challenges in photocatalytic ammonia synthesis are as follows: (1) the inert $N_2$ molecules and low solubility in aqueous solution make $N_2$ molecules difficult to be adsorbed and activated. (2) Only the light in a specific wavelength range is absorbed and utilized, while a large amount of light in the visible and infrared bands are wasted. Therefore, the efficiency of solar energy utilization and conversion is very low. To effectively utilize solar energy and increase the yield of photocatalytic ammonia synthesis, it is very important to develop efficient photocatalysts and reaction systems for ammonia synthesis.

Photocatalytic ammonia synthesis involves some basic processes, such as light capture, charge separation, and surface catalysis. Thus, the ideal photocatalysts are supposed to be compatible with proper band gap, highly efficient separation of electrons and holes, superior activation ability of $H_2O$ and $N_2$ molecules. At present, photocatalysts for ammonia synthesis are normally divided into inorganic photocatalysts (such as titanium dioxide ($TiO_2$)-based, bismuth (Bi)-based materials, etc.), bionic photocatalysts and new-type photocatalytic materials. Due to the excellent optical properties (e.g., narrow band gap to allow wide solar spectrum capture), $TiO_2$-based and Bi-based materials are the most widely studied inorganic materials in photocatalytic ammonia synthesis.

In 1977, G. N. Schrauzer and T. D. Guth systematically studied photocatalytic ammonia synthesis for the first time. They found that the inorganic $TiO_2$ material had a certain photocatalytic ammonia synthesis activity [114]. This pioneer work has aroused great interests, to investigate photocatalytic ammonia synthesis, especially for modification of $TiO_2$ material. For instance, Schrauzer

et al. prepared the $TiO_2$ photocatalysts doped with transition metals, such as Fe, Co, Ni, Cu, Cr, Mo, V, Pb, Au, Pd, Ag or Pt, for photocatalytic ammonia synthesis [114]. Amongst these dopants, the Fe, Co, Ni and Mo modified $TiO_2$ photocatalysts exhibited the best catalytic performance, which was ascribed to the predominance of rutile phase $TiO_2$ (10 – 95%) in these samples. Additionally, the introduction of defect sites and metal-oxide supports for $TiO_2$-based materials can also improve the activity of photocatalytic ammonia synthesis (Fig. 9a) [115].

In 2015, Zhang et al. first found that the BiOBr with abundant oxygen vacancy showed good photocatalytic performance of ammonia synthesis. The yield of ammonia synthesis reached 104.2 μmol $g^{-1}$ $h^{-1}$ without any sacrificial agents [116]. It was revealed that the oxygen vacancies of BiOBr with availability of localized electrons can activate the adsorbed $N_2$. Thus, it can efficiently produce ammonia by the interfacial electrons transferred from the excited BiOBr nanosheets (Fig. 9b).

As we know, $N_2$ molecules can be converted to ammonia under ambient conditions, driven by the nitrogenase enzyme. Biomimetic photocatalysts are prepared on the basis of the structure of nitrogenase enzyme, which exhibit promising performance in photocatalytic ammonia synthesis. For instance, Brown et al. isolated the nitrogenase MoFe-based protein from nitrogen-fixation bacteria, and integrated it with highly photosensitive CdS nanorods, to successfully fabricate a CdS nanorods/MoFe protein [117]. It can drive the reduction of $N_2$ to ammonia under ambient conditions. Kanatzidis et al. prepared the $Mo_2Fe_6S_8$-$Sn_2S_6$ chalcogel material for ammonia synthesis. The $Sn_2S_6$ chalcogel was employed as the light harvesting component, and the $Mo_2Fe_6S_8$ was used to provide the active sites

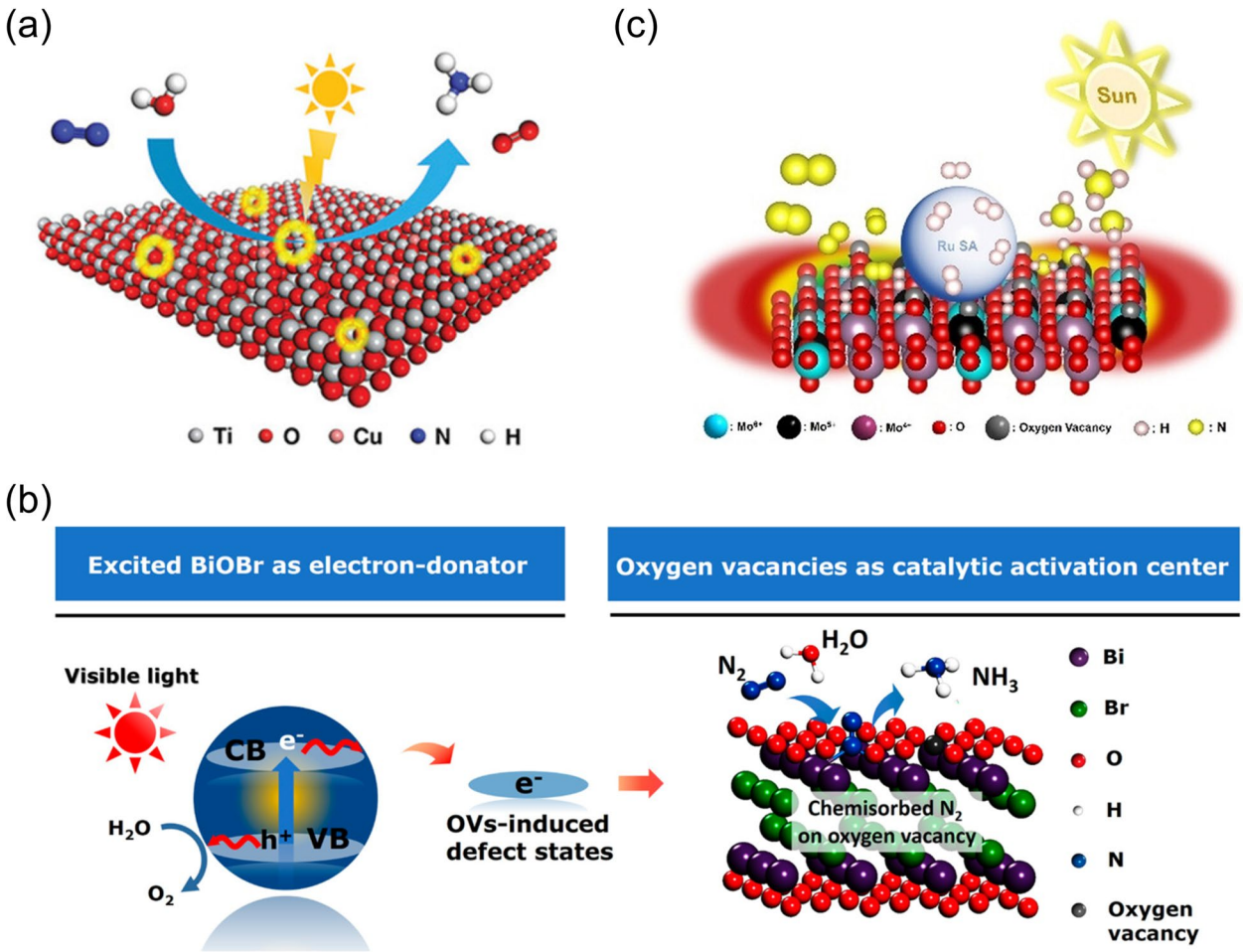


**Fig. 9** **a** Photocatalytic N2 fixation process on the surface of Cu-loaded ultrathin TiO2 nanosheets with oxygen (Ov). Reproduced with permission from ref. 115. Copyright (2019) Wiley–VCH Verlag GmbH & Co. KGaA, Weinheim. **b** Schematic diagram of photocatalytic ammonia synthesis over BiOBr catalysts. Reproduced with permission from ref. 116. Copyright (2015) American Chemical Society. **c** Schematic diagram of photocatalytic ammonia synthesis over Ru-SA/HxMoO3-y Catalyst. Reproduced with permission from ref. 120. Copyright (2022) Wiley–VCH Verlag GmbH & Co. KGaA, Weinheim

for nitrogen reduction. Thus, $Mo_2Fe_6S_8$-$Sn_2S_6$ chalcogel exhibited excellent photocatalytic activity and stability over a 72-h test period [118].

Recently, some emerging photocatalysts materials (such as layered double hydroxides (LDHs), single-atom catalysts (SACs), and polymer coordination materials) have been reported for photocatalytic ammonia synthesis. For example, Zhang et al. reported that hydrotalcite materials, such as CuCr, NiCr and ZnCr, had good photocatalytic performance of ammonia synthesis. The highest ammonia yield of CuCr hydrotalcite reached 184 μmol $L^{-1}$ [119]. In addition, Li et al. prepared the $H_xMoO_{3-y}$ support for atomically dispersed Ru-based catalyst (Ru-SA/$H_xMoO_{3-y}$), which achieved a photocatalytic ammonia synthesis rate of 4.0 mmol $g^{-1}$ $h^{-1}$ through the synergistic effect of $Ru_1$ and $Mo^{n+}$ dual sites (Fig. 9c) [120]. Jin et al. reported that the Zn-based coordination polymer materials can achieve an ammonia synthesis yield of 140 μmol $g^{-1}$ $h^{-1}$ [121].

Although many types of photocatalytic catalysts have been reported for ammonia synthesis, the yield of photocatalytic ammonia synthesis is far away from the requirement of industrial applications. To further improve the efficiency of photocatalytic ammonia synthesis, it is necessary to optimize the reaction system in all aspects, including photocatalysts, light trap systems, reaction systems, etc., so as to promote the development of photocatalytic technology for ammonia synthesis.

## 4 Ammonia utilization

As one of the largest bulk chemicals in the world, ammonia possesses a market size of 175 million tons and a market value of US$67 billion [122, 123]. In the past 100 years, the use of chemical fertilizers from ammonia has promoted the development of modern society. The fertilizer production accounts for 80% of the ammonia in 2022 (Fig. 10) [124]. The usage of fertilizer will continue to rise, to curb global hunger over the next three decades [125]. Besides, ammonia is also employed in industry, as a component of various nitrogen-containing compounds. To widen its synthetic utility, the efforts in organic synthesis and catalysis have been increasing continuously. To date, a series of various reactions (such as reductive amination, hydroaminomethylation, alkylation of alcohols, N-arylation, hydroamination, cyanation, aminocarbonylation, and so on) have been developed recently [126–130].

Traditionally, the direct utilization of ammonia as reagent in transition-metal catalysis is challenging, due to the stable Lewis acid–base adducts, facile ligand exchange and chemoselectivity. Despite these difficulties, the direct employment of ammonia as a nitrogen source in metal catalysis is highly economical and advantageous. Various transition metals (Au, Pd, Ru, Rh, Ir, Fe, and Cu) in combination with suitable ligands have been successfully applied to the ammonia reactions. It is anticipated that this trend of utilizing ammonia in catalytic reactions will intensify in the future [131].

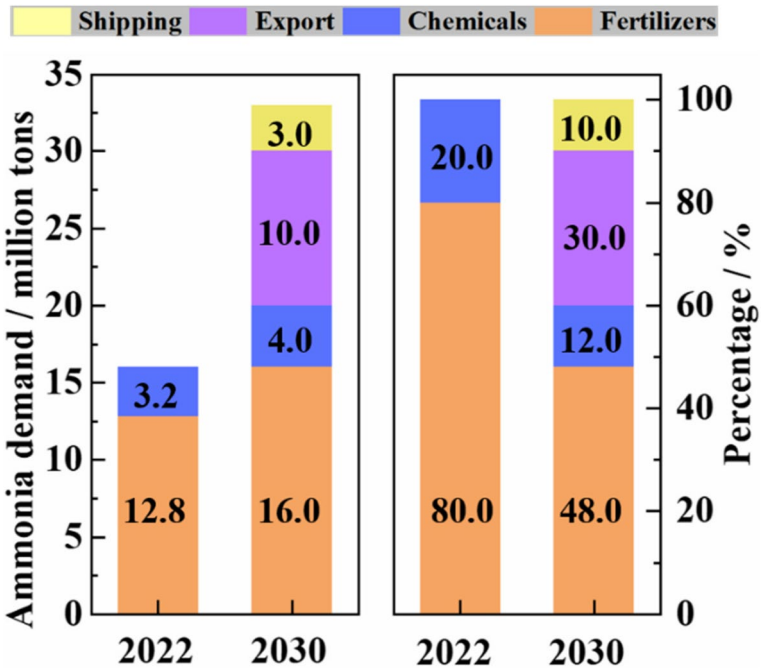


**Fig. 10** Ammonia demand in the US and its derived pathways in 2022 and 2030

Most recently, utilization of ammonia as an energy vector has attracted increasing attention, motivated by the global goals for net-zero carbon emissions. Ammonia is an idea hydrogen carrier, as it has a high hydrogen content (17.8 wt.%), high volumetric density (121 kg $H_2$ $m^{-3}$ at 10 bar), and easily liquefaction (8 bar at 25 °C). In addition, the high-capacity infrastructure and mature global transportation for ammonia allows the efficient storage and redistribution of ammonia, around the world, with the lowest economic cost. Today, the ammonia demand is dominated by the fertilizers (80%) and the remaining 20% is for chemical synthesis. As predicted, the demand pool of ammonia could be very different as soon as 2030. The 10% of ammonia would be used as fuel for shipping (Fig. 10) [132]. In 2040, the ammonia demand for shipping would be 15 million mt/annum, which is 1.5-fold than that of heavy fuel oil. Therefore, new energy roadmap for ammonia utilization is of the significance in the futuristic "ammonia economy", which includes ammonia decomposition for hydrogen production, direct ammonia fuel cells and ammonia combustion [133].

### 4.1 Ammonia decomposition

The ammonia can be decomposed into carbon-free hydrogen for further utilization ($2\ NH_3 = N_2 + 3\ H_2$, $\Delta H = 92.5$ kJ $mol^{-1}$). The ammonia decomposition is a endothermic reaction with entropy increment. The increase of reaction temperature under atmospheric pressure is beneficial for hydrogen production. Traditionally, the research on ammonia decomposition is strongly correlated to ammonia synthesis, due to the principle of microscopic reversibility. It suggests that under a given set of reaction conditions, the rate of ammonia decomposition can be expressed in term of the rate of ammonia synthesis in a linear relationship. However, the later studies found that the best catalyst for ammonia decomposition was not necessarily the optimal catalyst of ammonia synthesis, because the N-binding energies might vary greatly under different reaction conditions [134].

For example, Weinberg et al. [135] investigated the kinetics for ammonia decomposition, and demonstrated that the rate-determining step of ammonia decomposition on Ru(001) crystalline surface was significantly affected by the reaction temperatures at low ammonia pressures. The nitrogen recombination and desorption on the catalyst surface is the rate-determining step, when the reaction temperatures are lower than 650 K. The rate-determining step is the removal of the first hydrogen atom via breaking the N–H bond, when the reaction temperatures are higher than 750 K. Takahashi et al. [136] compared the reaction rate constants under the same reaction conditions. They illustrated the differences in the catalytic mechanism, by comparing the kinetic results with the pre-exponential factor and activation energies of each radical step. The rate-determining step of Ru-based catalysts in ammonia decomposition is nitrogen recombination, and the rate-determining step of Ni-based catalysts is N–H bond breaking.

Conventionally, numerous of catalysts for ammonia decomposition have been studied in Ru-based, Co-based and Fe-based catalysts [137]. The Ru-based catalysts is the most active catalysts for ammonia decomposition under low reaction temperatures [28]. However, the large-scale application of Ru-based catalysts is limited by high cost of ruthenium metal. The Ni-based catalysts are favored as an alternative to Ru-based catalysts, due to their low cost with satisfying activity. To date, the activities and stabilities for ammonia decomposition over the Ru-based and Ni-based catalysts have been enhanced by modulating the supports, promoters and preparation methods. The supports play an important role to affect size distribution, morphology and electronic state of the active metals. The promoters usually act as an electron supplier to promote the nitrogen recombination to accelerate the reaction rate. The preparation methods can improve catalytic performance of ammonia decomposition by enhancing metal-support interaction and regulating active metal particle size [138, 139].

For instance, Cha et al. reported that nanometer- and sub-nanometer-sized Ru particles were observed in their work [140]. The HAADF-STEM images of vacuum-calcined Ru/M-Y (M = H, Na, K, and Rb) catalysts revealed highly monodisperse Ru particles, while air-calcined catalysts showed considerably agglomerated and poorly dispersed Ru particles (Fig. 11a). The highly monodisperse Ru particles can facilitate the process of ammonia decomposition. Fang et al. prepared atom-dispersed Ru on MgO(111). The catalyst exhibits superior performance in ammonia decomposition. The increase of surface Ru concentration, correlated with increase in specific activity per metal site, clearly indicates synergistic metal sites in close proximity, akin to those bimetallic $N_2$ complexes in solution are required for the stepwise dehydrogenation of ammonia to $N_2/H_2$ (Fig. 11b) [141]. Kiya et al. fabricated a highly efficicient Ni/CaNH catalyst through an $NH_2$–vacancy-mediated Mars–van Krevelen mechanism [142]. They revealed that the Ni nanoparticles played an important role in promoting $NH^{2-}$-vacancy for ammonia decomposition (Fig. 11c). $Ni/Al_1Ce_aO_x$ catalysts was synthesized through one-pot anion-cation double hydrolysis by Quoc Cuong et al. It had an excellent activity, which was attributed to more surface oxygen vacancy and better $NH_3$ adsorption affinity (Fig. 11d) [143].

Although there are numerous efforts on efficient ammonia decomposition, it still remains great challenging, due to the economy and catalytic efficiency of the

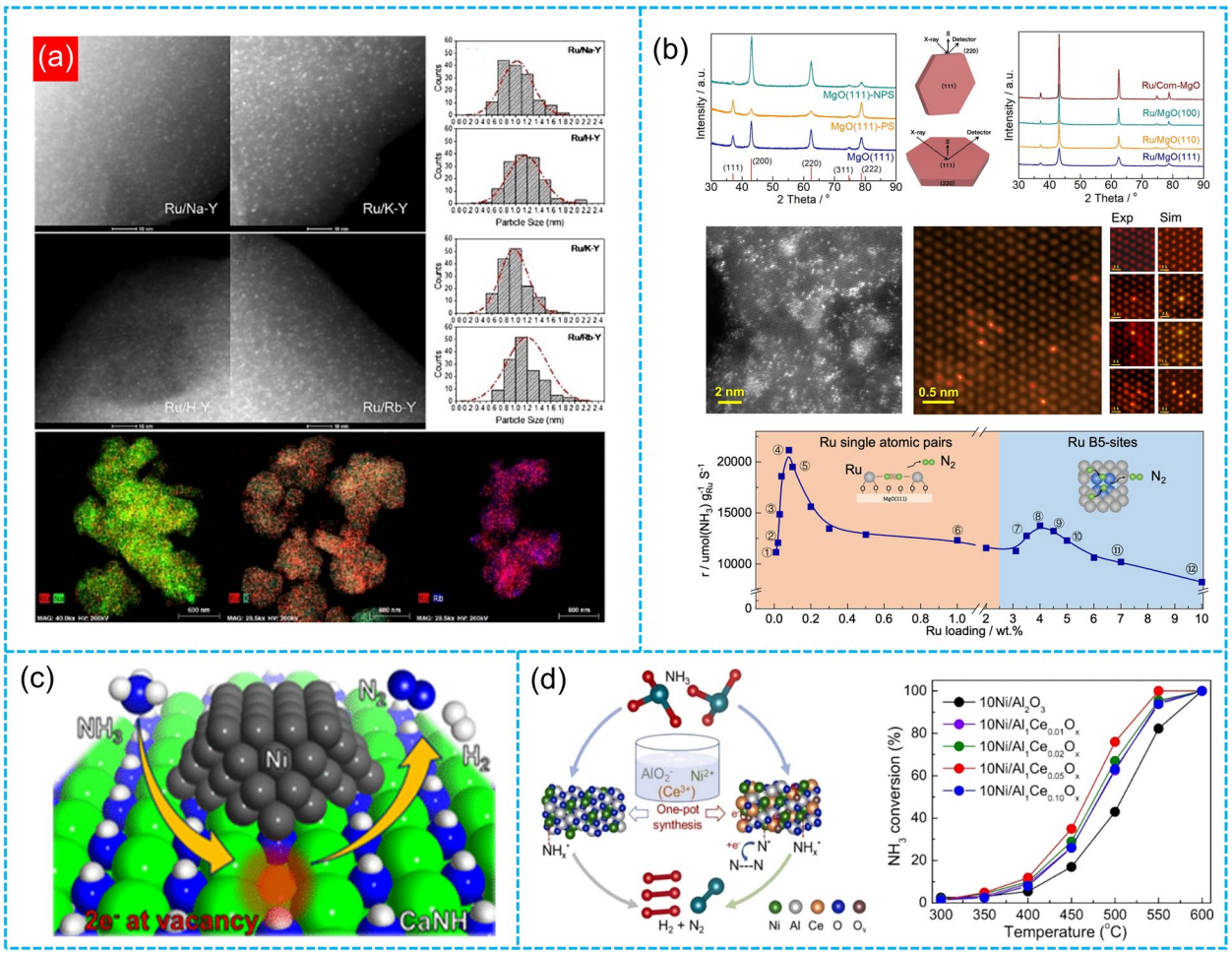


**Fig. 11** **a** TEM images and catalytic performance of Ru/Y catalysts. Reproduced with permission from ref. 140. Copyright (2021) Elsevier. **b** XRD patterns, TEM images and catalytic performance of Ru/MgO catalysts. Reproduced with permission from ref. 141. Copyright (2023) Nature Publishing Group. **c** Possible reaction pathway for ammonia decomposition over Ni/CaNH catalysts through an NH2- – vacancy-mediated Mars – van Krevelen mechanism. Reproduced with permission from ref. 142. Copyright (2021) American Chemical Society. **d** Catalytic performance of Ni/ Al1CeaOx catalysts. Reproduced with permission from ref. 143. Copyright (2022) Elsevier

catalysts. For Ru-based catalysts, minimizing the loading of active metals with high activities and long-term stabilities can effectively reduce the cost of catalysts. For Ni-based catalysts, they show satisfying activities for ammonia decomposition, while the stability of the catalysts is greatly limited by particle aggregation, sintering of active centers, and strong hydrogen inhibition [144–146]. It is urgent to increase the ammonia decomposition activity of Ni-based catalysts, and reduce the reaction temperature and energy consumption. Motivated by improving catalytic activity, the guidance for the catalysts is as follows [147]: (1) precise control of particle size/shape of active metals (e.g., Ru and Ni) to maximize the number of active sites; (2) addition of second metal for enhancing synergistic catalysis via structure stabilization and electronic effects; (3) introducing electronic and structural promoters/supports for activity promotion.

### 4.2 Ammonia fuel cells

Ammonia is a promising medium for hydrogen storage. It has well-established storage and transportation. Moreover, the notion of green ammonia from renewable energy is an emerging topic. It may open significant markets, and provide a pathway to decarbonize a variety of applications reliant on fossil fuels. Ammonia fuel cells can include direct ammonia fuel cell and indirect ammonia fuel cell. The indirect ammonia fuel cell is carried out by coupling ammonia decomposition and proton exchange membrane fuel cell for power generation (Fig. 12a) [148]. In the indirect ammonia fuel cell, ammonia can be fed to generate electricity with an excellent ammonia-to-electricity conversion.

The direct ammonia fuel cell can be divided into direct ammonia solid oxide fuel cell (DA-SOFC) and direct ammonia alkaline exchange membrane fuel cell

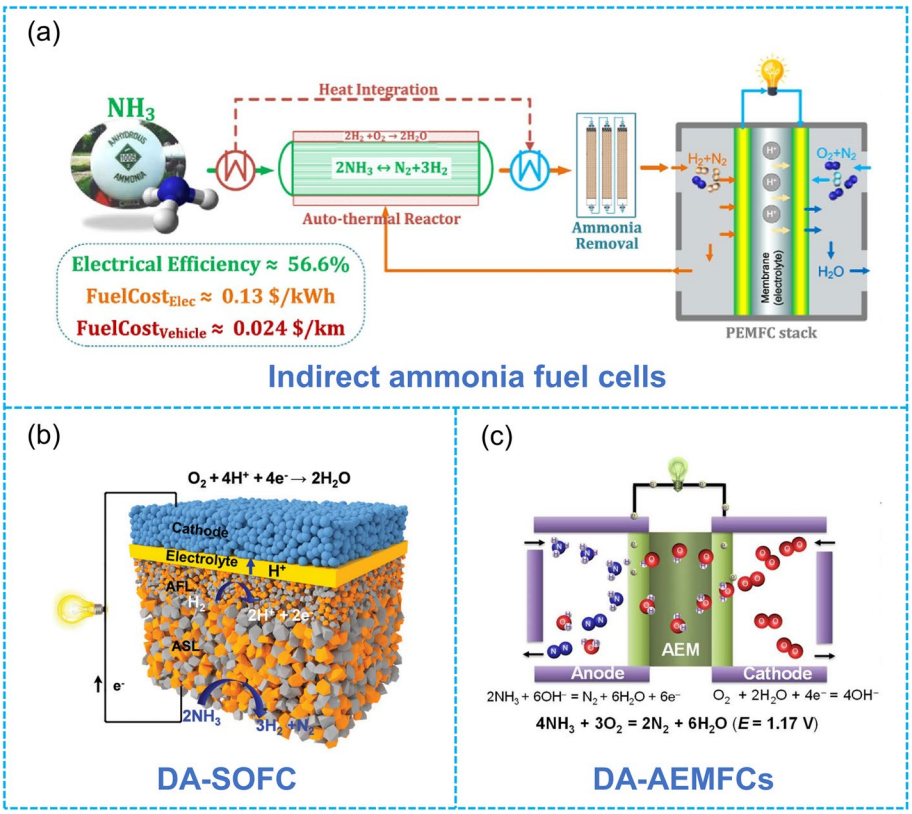


**Fig. 12** Schematic of (**a**) indirect ammonia fuel cells. Reproduced with permission from ref. 148. Copyright (2022) Elsevier. **b** Direct ammonia solid oxide fuel cell. Reproduced with permission from ref. 149. Copyright (2022) Royal Society of Chemistry. **c** Direct ammonia alkaline exchange membrane fuel cell. Reproduced with permission from ref. 150. Copyright (2021) Royal Society of Chemistry

(DA-AEMFC), as shown in Fig. 12b and c [149, 150]. The operating temperature of DA-SOFC is generally 600–1000 °C with high energy efficiency (over 60%), low polarization loss. On the other hand, DA-AEMFC work under similar principles as alkaline fuel cells, because they also work by transfer of $OH^-$ ions through electrolyte and operate at a low temperature range of approximately 50–120 °C. In the DA-AEMFC, oxygen is introduced at the cathodic component, where a reaction with water occurs to generate $OH^-$ ions. The $OH^-$ ions are then transported across an alkaline-based membrane to the anodic side, where they react with ammonia to produce nitrogen and water.

DA-SOFCs can be sorted into two categories in accordance with the type of electrolyte: oxygen ion conducting electrolyte-based SOFCs (DA-SOFC-O) and proton conducting electrolyte-based SOFCs (DA-SOFC-H). The conventional DA-SOFC-O has been widely developed with mature preparation technology. Due to the working temperatures in range of 800 and 1000 °C, the stability of materials is the major concern for DA-SOFC-O. The issues (such as electrode decomposition, sintering, diffusion between electrolyte and electrode material, and stress caused by the difference of thermal expansion coefficient) always result in the degradation of the cell performance after long-term operation.

In contrast, the DA-SOFC-H can effectively avoid the increase of ohmic resistance, due to the lower activation energy of proton conduction. It can operate under lower temperatures (500–800 °C), which possesses great potential for commercial applications. Recently, efforts have also been made in DA-SOFC-H. Zhang et al. [149] used 7 μm-thick BZCYYb as the electrolyte, and Fe–Ni-BZCYYb and BSCF as the anode and cathode, respectively, to prepare the cell unit. The cell obtained a peak power density of 1.609 $Wcm^{-2}$ at 700 °C, which shows the best performance reported in literatures so far. This indicates that the performance of DA-SOFC-H at low temperatures has surpassed the best performance of DA-SOFC-O reported by Meng et al. (peak power density of 1.19 $Wcm.^{-2}$ at 650 °C) [151].

Previous studies have shown that the low ratio of ammonia/hydrogen performance of DA-SOFC at low temperatures is a common issue in DA-SAOFCs. Aoki et al. [152] reported a power density ratio of 69.4–71.6% for ammonia to hydrogen at 550–600 °C. This value

was improved by He et al. [153] to 70.5–80.9%. The low ammonia/hydrogen ratio was mainly caused by inefficient ammonia decomposition at anode under low temperatures. It is challenging for performance durability and material fabrication in DA-SOFCs, to endure such high temperatures for an extensive period of time. Moreover, on the catalysts, it is extremely important to avoid chemical compatibility issues in the long-term operation.

To date, the development of DA-AEMFCs is at an earlier stage, compared with hydrogen fuel cells. This is mainly because the slow reaction kinetics of ammonia oxidation reaction (AOR) usually requires a high overpotential (> 0.4 V), which increases the energy requirement for the reaction, and lowers the output performance. Additionally, the intermediate substances ($^{*}$N, $^{*}$NO), adsorbed on the catalyst surface to occupy the active sites, may lead to the catalyst poisoning [154]. At present, the commonly used AOR catalysts are noble metal catalysts (for example, Pt-based catalysts) and non-precious metal catalysts (such as Ni, and Cu based catalysts). However, the poor catalyst activity, selectivity and stability, and the high cost of noble metals are the main factors, to limit commercial application of DA-AEMFCs. The search for good low-cost anode and cathode materials as well as new electrolyte materials, is still a topic of interest. The anionic polymer membrane, the preparation process of membrane electrodes and the flow channel design of bipolar plate, are also the key issues and challenges, to enhance the performance of DA-AEMFC. With the breakthrough of these challenges, the direct ammonia fuel cell will possess a broad prospect and application market in the future.

### 4.3 Ammonia combustion

Ammonia could be directly used as a fuel for gas furnaces, turbines and engines, to produce clean power with only emission of $N_2$ and $H_2O$. It is conducive to building a clean power system and solving the problem of carbon emissions [155]. The attractive advantage of ammonia as a fuel is that it can be achieved by retrofitting existing combustion equipment [147]. However, there are several challenges in ammonia combustion for large-scale application, mainly due to its poor combustion features and $NO_x$ emissions. Compared with typical hydrocarbon fuels, ammonia has lower calorific value and maximum laminar burning velocity, as well as lower flame temperature and longer ignition delay time. Besides, the flammability of ammonia is also low, mainly reflected in its narrower flammability range and higher ignition temperature [156]. Another key issue of ammonia combustion is the risk of high $NO_x$ emissions [157]. Unlike common hydrocarbon fuels, the nitrogen content of ammonia is as high as 82%, and NO is mainly generated through fuel-type mechanisms during combustion. Many studies have shown that the $NO_x$ emission level from ammonia combustion is at least an order of magnitude higher than that of common hydrocarbon fuels. For example, using pure ammonia, the volume fractions of outlet NO from a 50 kW micro gas turbine was as high as $1000 \times 10^{-6}$ (16% $O_2$) [157].

It is critical to improve combustion intensity for applications of ammonia combustion in gas turbine and engine. At present, strategies, proposed to enhance ammonia combustion, can be generally subdivided into the following three ways [155]: (1) blending ammonia with other higher activity fuels like hydrogen [158–160], methane [161–166], syngas [167, 168], oxygenated fuels [169–172]; (2) using oxygen-enriched mixtures replacing air to enhance oxidizer [173–175]; (3) increasing turbulence to increase the flame velocity relative to the laminar burning velocity (Fig. 13a-c) [155, 176–179].

The blending with hydrogen significantly increases the flame velocity of ammonia, due to its high reactivity and adiabatic flame temperature. Hydrogen is found to be the most effective combustion promoter for ammonia. The 10% (by vol.) or less hydrogen is sufficient to significantly affect flame stability [180–182] Additionally, methane is found to be the least effective combustion promoter [155]. Some researchers found that the temperature of the adiabatic flame increased with the increase of oxygen content. This is the main reason of the acceleration of laminar burning velocity in the oxygen-rich flame [173]. Hence, increasing oxygen content is considered another valid approach, to enhance reactivity of ammonia combustion [155].

$NO_x$ reduction is still the main challenge for the utilization of ammonia in practical combustion devices [155]. The substantial evidence has shown that the lean premixed ammonia-air flames produce extremely large NO emissions, sometimes reaching thousands of ppm [155], so do ammonia-methane and ammonia-hydrogen fuel blends. Therefore, it is difficult to directly use ammonia as a drop-in fuel in current gas turbines. Motivated by this, two-stage combustion is proposed as an effective strategy for gas turbine combustors fueled by ammonia or its blends (Fig. 13d) [183]. For example, Okafor et al. [184] reported a two-stage combustion fueled by pure ammonia at 3 bar, with a thermal power of 32 kW, in which $NO_x$ emissions were limited to 42 ppm and the combustion efficiency reached 99.5%. In two-staged combustion, the primary rich stage equivalence ratio is of great importance for NO emissions [183]. Another fact, highlighted in many studies [156], is that the increase of pressure generally reduces emissions of NO and unburned ammonia. This is beneficial to power generation, as industrial

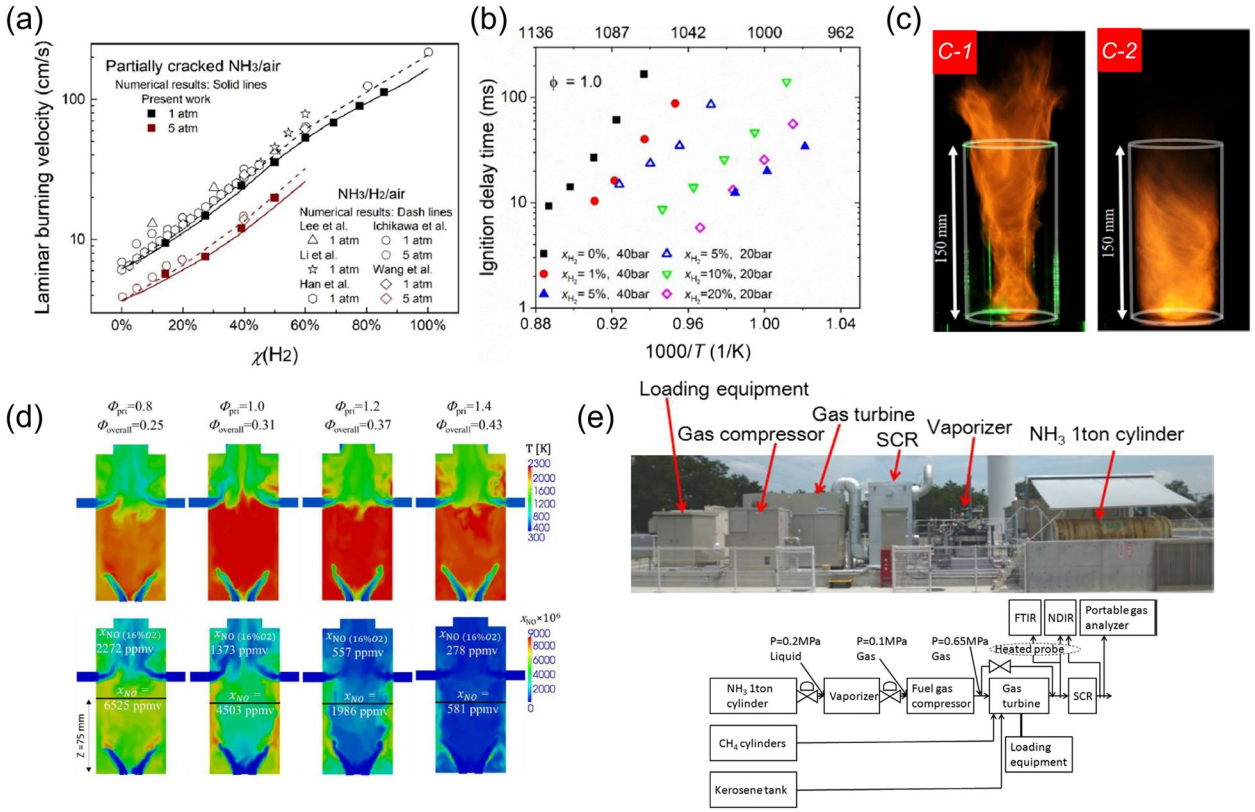


**Fig. 13** **a** The laminar burning velocity of two blends of NH3-H2-O2-N2 mixtures versus hydrogen mole fraction at Φ = 1 and *P* = 1 atm and 5 atm. Reproduced with permission from ref. 155. Copyright (2022) Elsevier. **b** Effect of the NH3/H2 ratio on the measured ignition delay time for the stoichiometric mixtures. Reproduced with permission from ref. 178. Copyright (2019) Elsevier. **c** Photographs of (c-1) a pure liquid ammonia spray flame and (c-2) a liquid ammonia spray flame co-fired with methane. Reproduced with permission from ref. 179. Copyright (2021) Elsevier. **d** 2-D simulated temperature distributions (top row) and NO mole fraction (bottom row) in a two-stage swirl combustor fueled by ammonia-methane-air mixtures with different equivalence ratios. Reproduced with permission from ref. 184. Copyright (2020) Elsevier. **e** Photo and schematic diagram of the experimental facility of NH3–air and NH3–CH4–air combustion gas turbine power generation. Reproduced with permission from ref.157. Copyright (2017) Elsevier

gas turbines operate at high pressure to increase efficiency and power density.

Although staged combustion exhibits excellent performance in abating $NO_x$ emissions, it cannot be adopted on a large scale in the near future. Many researchers [181, 182, 185] also found that the sufficiently lean premixed ammonia-hydrogen swirl flames showed a performance of NO amount < 100 ppm in their exhaust. The NO mitigation depended on the ammonia fraction in ammonia-hydrogen blend, as well as the pressure. It is worth noting that this strategy is not applicable to lean premixed pure ammonia flames or ammonia-methane flames [186]. Another strategy, already adopted in practice, is that installs a selective catalytic reduction (SCR) system in downstream of the turbine, which can reduce $NO_x$ emissions below 10 ppm (Fig. 13e). By pairing with SCR, the Fukushima Renewable Energy Institute of the National Institute of Advanced Industrial Science and Technology (FREA-AIST) reported successful power generation, using gas turbine fueled by ammonia [157]. Other $NO_x$ reduction strategies are still being explored, including extremely lean burning, flameless combustion, and humidification [155]. In the future, electrocatalytic NOx reduction may also be a possible technology, to promote regeneration and cyclic utilization of ammonia in the engine/turbine systems.

## 5 Concluding remarks and future perspectives

### 5.1 Concluding remarks

Hydrogen production, ammonia synthesis and ammonia utilization are the key steps in energy storage and utilization via ammonia. The hydrogen production employ carbon resources and water as feedstocks. The Group VIII metals, such as Ru, Rh, Pt, Ir, Ni, and Co, are active for reforming of carbon feedstocks. The Ni-based catalysts are the most commonly used in industry, due to its good activity and low cost. However, the Ni-based catalysts encounter two major challenges, i.e., carbon formation

and sintering of Ni particles. Hydrogen production from water is more environmentally friendly than that from carbon feedstocks. During water electrolysis, the Pt-based catalysts are found to be efficient for HER. But, due to the high cost, it is necessary to improve the catalytic performance with low-Pt loading. In addition, photonic energy can also be employed to produce hydrogen from water via photocatalytic process, but it is low in efficiency.

In ammonia synthesis, the industrial HB process obeys thermocatalytic pathway to realize large-scale production of ammonia. The renewable energy-driven HB process can promote the miniaturized production of ammonia with low energy consumption. It is essential to develop efficient catalysts with mild reaction conditions for the production. The ammonia synthesis via electrocatalysis can bypass the process of hydrogen production. But low solubility of nitrogen molecule and competition of HER result in low rate of ammonia synthesis and low Faraday efficiency. The photocatalytic synthesis of ammonia can directly convert solar energy into chemical energy without the $CO_2$ emissions. However, it is still a great challenge to realize large-scale production, due to the extremely low efficiency of solar energy utilization and low yield of ammonia synthesis.

To explore high-efficiency processes of ammonia utilization, the ammonia decomposition possesses an opportunity for potential use of ammonia, as a carrier of hydrogen energy. However, it remains challenging to develop efficient and eco-friendly catalysts for ammonia decomposition under low temperatures. The ammonia fuel cells can generate electricity with an excellent conversion of ammonia. But they still suffer from many obstacles (such as sluggish kinetics, low stability, etc.) in long-term operation. The ammonia combustion can be used in gas furnaces, turbines and engines, to reduce consumption of fossil fuels. However, it is needed to lower the concentration of $NO_x$ species during the process of ammonia combustion.

### 5.2 Future perspectives

Hydrogen production has been studied for many years. In the future, green methods for hydrogen production will help to significantly reduce consumption of fossil fuels and lower environmental pollution. Although ammonia synthesis via HB process has been used in large-scale industrial applications, it is urgent to improve the HB process with mild reaction conditions. It is also very necessary to develop high-efficiency photocatalytic/electrocatalytic processes for ammonia synthesis. In ammonia utilization, ammonia can be applied to produce agricultural fertilizers and industrial chemicals. More significantly, it should be rationally utilized in ammonia decomposition, ammonia fuel cells and ammonia combustion, to optimize energy structure in the world. We consider that there is a great need to develop new approaches and high-efficiency processes in these fields.

In addition to the hydrogen production, ammonia synthesis and ammonia utilization, ammonia separation is also an important aspect in the process of energy storage and utilization via ammonia. It is due to the fact that the purity of ammonia can significantly impact on subsequent ammonia utilization. At present, the ammonia separation is realized by physical condensation after industrial ammonia synthesis. However, the efficiency of physical condensation is unsatisfying, because of the vapor–liquid equilibrium of ammonia. Liquid absorption and solid adsorption are further proposed routes for ammonia separation [187, 188]. Liquid absorption makes use of different solubilities of gases in liquid solvents, and solid adsorption depends on different adsorption capacities of gases on solid adsorbents. In the future, we speculate that integration of the physical condensation with liquid absorption and/or solid adsorption will be an important development direction to obtain high-purty ammonia in industry, because it can considerably save cost and energy consumption.

Based on these future perspectives, energy storage and utilization via ammonia will solve a series of crucial issues for developments of hydrogen energy and renewable energies. In modern society, hydrogen storage and transportation are bottleneck problems in large-scale application. Ammonia, as a carrier of hydrogen, possesses mature technologies of storage and transportation, to overcome the bottleneck problems and provide hydrogen energy. In storage and utilization of renewable energies, ammonia will also play a key role. Renewable energy sources (such as solar, wind and hydropower) can be converted into chemical energy via ammonia. They can be released by the processes of ammonia fuel cells, ammonia combustion, etc., to realize zero-carbon emissions of energy storage and utilization. We expect that the energy storage and utilization via ammonia will promote energy decarbonization, and build a society of carbon-free energy in the future.

**Acknowledgements**

This work is supported by the National Natural Science Foundation of China (Nos. 22221005, 22278078, 22178058 and 22108037), and National Key R&D Program of China (Nos. 2022YFB4002602 and 2022YFB4003701).

**Authors' contributions**

LJ and XP conceived this review. CC, YZ and HF wrote the original manuscript. LJ and XP edited and revised the manuscript. All authors contributed equally on all revisions and approved the final manuscript.

## Declarations

### Competing interests

Lilong Jiang is a member of the editorial board of this journal. He was not involved in the editorial review or the decision to publish this article. All authors declare that there are no competing interests.

Received: 22 July 2023 Revised: 30 September 2023 Accepted: 6 October 2023
Published online: 10 November 2023

### References

1. Guo J, Chen P (2017) Catalyst: $NH_3$ as an energy carrier. Chem 3:709–712
2. Nagaoka K, Eboshi T, Takeishi Y et al (2017) Carbon-free $H_2$ production from ammonia triggered at room temperature with an acidic $RuO_2$/γ-$Al_2O_3$ catalyst. Sci Adv 3:e1602747
3. Marakatti VS, Gaigneaux EM (2020) Recent advances in heterogeneous catalyst for ammonia synthesis. ChemCatChem 12:5838–5857
4. Foster SL, Bakovic SIP, Duda RD et al (2018) Catalysts for nitrogen reduction to ammonia. Nat Catal 1:490–500
5. Wang Q, Guo J, Chen P (2019) Recent progress towards mild-condition ammonia synthesis. J Energy Chem 36:25–36
6. Hattori M, Iijima S, Nakao T et al (2020) Solid solution for catalytic ammonia synthesis from nitrogen and hydrogen gases at 50 °C. Nat Commun 11:2001
7. Smith C, Hill AK, Torrente-Murciano L (2020) Current and future role of Haber-Bosch ammonia in a carbon-free energy landscape. Energy Environ Sci 13:331–344
8. Megía PJ, Vizcaíno AJ, Calles JA et al (2021) Hydrogen production technologies: from fossil fuels toward renewable sources. A mini review. Energy Fuels 35:6403–16415
9. Ml Yu, Wang K, Vredenburg H (2021) Insights into low-carbon hydrogen production methods: green, blue and aqua hydrogen. Int J Hydrogen Energy 40:21261–21273
10. Chisalita DA, Petrescu L, Cormos CC (2020) Environmental evaluation of european ammonia production considering various hydrogen supply chains. Renew Sust Energ Rev 130:109964
11. El-Shafie M, Kambara S (2023) Recent advances in ammonia synthesis technologies: toward future zero carbon emissions. Int J Hydrogen Energy 48:11237–11273
12. Zhang HF, Wang LG, Herle JV et al (2020) Techno-economic comparison of green ammonia production processes. Appl Energy 259:114135
13. Anwar S, Khan F, Zhang YH et al (2021) Recent development in electrocatalysts for hydrogen production through water electrolysis. Int J Hydrogen Energy 46:32284–32317
14. Nishiyama H, Yamada T, Nakabayashi M et al (2021) Photocatalytic solar hydrogen production from water on a 100–$m^2$ scale. Nature 598:304–307
15. Liu GY, Sheng Y, Ager JW et al (2019) Research advances towards large-scale solar hydrogen production from water. Energy Chem 1:100014
16. Humphreys J, Lan R, Tao S (2021) Development and recent progress on ammonia synthesis catalysts for Haber-Bosch process. Adv Energy Sustainability Res 2:2000043
17. Wang M, Khan MA, Mohsin I et al (2021) Can sustainable ammonia synthesis pathways compete with fossil-fuel based Haber-Bosch processes? Energy Environ Sci 14:2535–2548
18. Singh AR, Rohr BA, Schwalbe JA et al (2017) Electrochemical ammonia synthesis-the selectivity challenge. ACS Catal 7:706–709
19. Jiao F, Xu BJ (2017) Electrochemical ammonia synthesis and ammonia fuel cells. Adv Mater 31:1805173
20. Zhang S, Zhao YX, Shi R et al (2019) Photocatalytic ammonia synthesis: recent progress and future. Energy Chem 1:100013
21. Ithisuphalap K, Zhang HG, Guo L et al (2018) Photocatalysis and photoelectrocatalysis methods of nitrogen reduction for sustainable ammonia synthesis. Small Methods 3:1800352
22. Wang XY, Peng XB, Chen W et al (2020) Insight into dynamic and steady-state active sites for nitrogen activation to ammonia by cobalt-based catalyst. Nat Commun 11:653
23. Shen HD, Choi C, Masa J et al (2021) Electrochemical ammonia synthesis: mechanistic understanding and catalyst design. Chem 7:1708–1754
24. Chen XZ, Li N, Kong ZZ et al (2018) Photocatalytic fixation of nitrogen to ammonia: state-of-the-art advancements and future prospects. Mater Horiz 5:9–27
25. Chang F, Gao WB, Guo JP et al (2021) Emerging materials and methods toward ammonia-based energy storage and conversion. Adv Mater 33:2005721
26. Aziz M, Wijayanta AT, Nandiyanto ABD (2020) Ammonia as effective hydrogen storage: a review on production. Storage Utilization Energies 13:3062
27. Valera-Medina A, Amer-Hatem F, Azad AK et al (2021) Review on ammonia as a potential fuel: from synthesis to economics. Energy Fuels 35:6964–7029
28. Mukherjee S, Devaguptapu SV, Sviripa A et al (2018) Low-temperature ammonia decomposition catalysts for hydrogen generation. Appl Catal B Environ 226:162–181
29. Jeerh G, Zhang MF, Tao SW (2021) Recent progress in ammonia fuel cells and their potential applications. J Mater Chem A 9:727–752
30. Cai T, Zhao D, Gutmark E (2023) Overview of fundamental kinetic mechanisms and emission mitigation in ammonia combustion. Chem Eng J 458:141391
31. Global hydrogen review 2022. International Energy Agency. https://www.iea.org/reports/global-hydrogen-review-2022. Accessed Sept 2022
32. Navarro RM, Pena MA, Fierro JLG (2007) Hydrogen production reactions from carbon feedstocks: fossil fuels and biomass. Chem Rev 107:3952–3991
33. Liu Z, Grinter DC, Lustemberg PG et al (2016) Dry reforming of methane on a highly-active Ni-$CeO_2$ catalyst: effects of metal-support Interactions on C-H bond breaking. Angew Chem Int Ed 55:7455–7459
34. Wang Y, Li L, Li G et al (2023) Synergy of oxygen vacancies and $Ni^0$ species to promote the stability of a Ni/$ZrO_2$ catalyst for dry reforming of methane at low temperatures. ACS Catal 13:6486–6496
35. Kim SM, Abdala PM, Margossian T et al (2017) Cooperativity and dynamics increase the performance of NiFe dry reforming catalysts. J Am Chem Soc 139:1937–1949
36. Koike M, Li D, Nakagawa Y et al (2012) A highly active and coke-resistant steam reforming catalyst comprising uniform nickel-iron alloy nanoparticles. Chemsuschem 5:2312–2314
37. Long H, Xu Y, Zhang X et al (2013) Ni-Co/Mg-Al catalyst derived from hydrotalcite-like compound prepared by plasma for dry reforming of methane. J Energy Chem 22:733–739
38. Yu X, Chu W, Wang N et al (2011) Hydrogen production by ethanol steam reforming on NiCuMgAl catalysts derived from hydrotalcite-like precursors. Catal Letters 141:1228–1236
39. Feyen M, Weidenthaler C, Guttel R et al (2011) High-temperature stable, iron-based core-shell catalysts for ammonia decomposition. Chem Eur J 17:598–605
40. Park JC, Lee HJ, Kim JY et al (2010) Catalytic hydrogen transfer of ketones over Ni@$SiO_2$ yolk-shell nanocatalysts with tiny metal cores. J Phys Chem C 114:6381–6388
41. Liang D, Wang Y, Chen M et al (2023) Dry reforming of methane for syngas production over attapulgite-derived MFI zeolite encapsulated bimetallic Ni-Co catalysts. Appl Catal B 322:122088
42. Akri M, Zhao S, Li X et al (2019) Atomically dispersed nickel as coke-resistant active sites for methane dry reforming. Nat Commun 10:5181
43. Meng H, Yang Y, Shen T et al (2023) A strong bimetal-support interaction in ethanol steam reforming. Nat Commun 14:3189
44. Qin T, Yuan S (2023) Research progress of catalysts for catalytic steam reforming of high temperature tar: a review. Fuel 331:125790
45. Lin F, Chen Z, Gong H et al (2023) Oxygen vacancy induced strong metal-support interactions on Ni/$Ce_{0.8}Zr_{0.2}O_2$ nanorod catalysts for promoting steam reforming of toluene: experimental and computational studies. Langmuir 39:4495–4506
46. Ursua A, Gandia LM, Sanchis P (2012) Hydrogen production from water electrolysis: current status and future trends. Proc IEEE Inst Electr Electron Eng 100:410–426

47. Li K, Li Y, Wang Y et al (2018) Enhanced electrocatalytic performance for the hydrogen evolution reaction through surface enrichment of platinum nanoclusters alloying with ruthenium in situ embedded in carbon. Energy Environ Sci 11:1232–1239
48. Cheng N, Stambula S, Wang D et al (2016) Platinum single-atom and cluster catalysis of the hydrogen evolution reaction. Nat Commun 7:13638
49. Xie J, Zhang H, Li S et al (2013) Defect-rich $MoS_2$ ultrathin nanosheets with additional active edge sites for enhanced electrocatalytic hydrogen evolution. Adv Mater 25:5807–5813
50. Faber MS, Dziedzic R, Lukowski MA et al (2014) High-performance electrocatalysis using metallic cobalt pyrite ($CoS_2$) micro- and nanostructures. J Am Chem Soc 136:10053–10061
51. Chang J, Li S, Li G et al (2016) Monocrystalline $Ni_{12}P_5$ hollow spheres with ultrahigh specific surface areas as advanced electrocatalysts for the hydrogen evolution reaction. J Mater Chem A 4:9755–9759
52. Popczun EJ, Read CG, Roske CW et al (2014) Highly active electrocatalysis of the hydrogen evolution reaction by cobalt phosphide nanoparticles. Angew Chem Int Ed 53:5427–5430
53. Wang Y, Hao S, Liu X et al (2020) Ce-doped $IrO_2$ electrocatalysts with enhanced performance for water oxidation in acidic media. ACS Appl Mater Interfaces 12:37006–37012
54. Wang J, Xi C, Wang M et al (2020) Laser-generated grain boundaries in ruthenium nanoparticles for boosting oxygen evolution reaction. ACS Catal 10:12575–12581
55. Jiang Y, Dong K, Lu Y et al (2020) Bimetallic oxide coupled with B-doped graphene as highly efficient electrocatalyst for oxygen evolution reaction. Sci China Mater 63:1247–1256
56. Li X, Wang Y, Wang J et al (2020) Sequential electrodeposition of bifunctional catalytically active structures in $MoO_3$/Ni-NiO composite electrocatalysts for selective hydrogen and oxygen evolution. Adv Mater 32:2003414
57. Zhao C, Li B, Zhao M et al (2020) Precise anionic regulation of NiFe hydroxysulfide assisted by electrochemical reactions for efficient electrocatalysis. Energy Environ Sci 13:1711–1716
58. Wang Z, Li C, Domen K (2019) Recent developments in heterogeneous photocatalysts for solar-driven overall water splitting. Chem Soc Rev 48:2109–2125
59. Mu L, Zhao Y, Li A et al (2016) Enhancing charge separation on high symmetry $SrTiO_3$ exposed with anisotropic facets for photocatalytic water splitting. Energy Environ Sci 9:2463–2469
60. Sun S, Wang W, Li D et al (2014) Solar light driven pure water splitting on quantum sized $BiVO_4$ without any cocatalyst. ACS Catal 4:3498–3503
61. Rahman ZU, Wei N, Feng M et al (2019) $TiO_2$ hollow spheres with separated Au and $RuO_2$ co-catalysts for efficient photocatalytic water splitting. Int J Hydrog Energy 44:13221–13231
62. Lee G, Anandan S, Masten SJ et al (2016) Photocatalytic hydrogen evolution from water splitting using Cu doped ZnS microspheres under visible light irradiation. Renew Energ 89:18–26
63. Liu J, Liu Y, Liu N et al (2015) Metal-free efficient photocatalyst for stable visible water splitting via a two-electron pathway. Science 347:970–974
64. Wang Z, Wang L (2018) Progress in designing effective photoelectrodes for solar water splitting. Chinese J Catal 39:369–378
65. Cooper JK, Gul S, Toma FM et al (2014) Electronic structure of monoclinic $BiVO_4$. Chem Mater 26:5365–5373
66. Higashi T, Nishiyama H, Nandal V et al (2022) Design of semitransparent tantalum nitride photoanode for efficient and durable solar water splitting. Energy Environ Sci 15:4761–4775
67. Wang G, Wang H, Ling Y et al (2011) Hydrogen-treated $TiO_2$ nanowire arrays for photoelectrochemical water splitting. Nano Lett 11:3026–3033
68. Xu F, Sun L (2011) Solution-derived ZnO nanostructures for photoanodes of dye-sensitized solar cells. Energy Environ Sci 4:818–841
69. Zhang H, Li D, Byun WJ et al (2020) Gradient tantalum-doped hematite homojunction photoanode improves both photocurrents and turn-on voltage for solar water splitting. Nat Commun 11:4622
70. Cho IS, Lee CH, Feng Y et al (2013) Codoping titanium dioxide nanowires with tungsten and carbon for enhanced photoelectrochemical performance. Nat Commun 4:1723
71. Li C, Chen M, Xie Y et al (2022) Boosting the solar water oxidation performance of $BiVO_4$ photoanode via non-stoichiometric ratio drived surface reconstruction. J Power Sources 528:231242
72. Dong G, Yan L, Bi Y (2023) Advanced oxygen evolution reaction catalysts for solar-driven photoelectrochemical water splitting. J Mater Chem A 11:3888–3903
73. Zhang B, Wang L, Zhang Y et al (2018) Ultrathin FeOOH nanolayers with abundant oxygen vacancies on $BiVO_4$ photoanodes for efficient water oxidation. Angew Chem Int Ed 57:2248–2252
74. Cai L, Zhao J, Li H et al (2016) One-step hydrothermal deposition of Ni:FeOOH onto photoanodes for enhanced water oxidation. ACS Energy Lett 1:624–632
75. Shi Y, Yu Y, Yu Y et al (2018) Boosting photoelectrochemical water oxidation activity and stability of Mo-doped $BiVO_4$ through the uniform assembly coating of NiFe-phenolic networks. ACS Energy Lett 3:1648–1654
76. Kim TW, Choi KS (2014) Nanoporous $BiVO_4$ photoanodes with dual-layer oxygen evolution catalysts for solar water splitting. Science 343:990–994
77. Marakatti VS, Gaigneaux EM (2020) Recent advances in heterogeneous catalysis for ammonia synthesis. ChemCatChem 12:5838–5857
78. Zhou Y, Wang C, Peng X et al (2022) Boosting efficient ammonia synthesis over atomically dispersed Co-based catalyst via the modulation of geometric and electronic structures. CCS Chem 4:1758–1769
79. Zheng J, Jiang L, Lyu Y et al (2021) Green synthesis of nitrogen-to-ammonia fixation: past, present, and future. Energy Environ Mater 5:452–457
80. Liu H (2014) Ammonia synthesis catalyst 100 years: practice, enlightenment and challenge. Chinese J Catal 35:1619–1640
81. Chang F, Tezsevin I, de Rijk JW et al (2022) Potassium hydride-intercalated graphite as an efficient heterogeneous catalyst for ammonia synthesis. Nat Catal 5:222–230
82. Zhou Y, Xu C, Tan Z et al (2022) Integrating dissociative and associative routes for efficient ammonia synthesis over a TiCN-promoted Ru-based catalyst. ACS Catal 12:2651–2660
83. Mao C, Yu L, Li J et al (2018) Energy-confined solar thermal ammonia synthesis with K/Ru/$TiO_{2-x}H_x$. Appl Catal B-Environ 224:612–620
84. Zhou Y, Sai Q, Tan Z et al (2022) Highly efficient subnanometer Ru-based catalyst for ammonia synthesis via an associative mechanism. Chin J Chem Eng 43:177–184
85. Zheng J, Liao F, Wu S et al (2019) Efficient non-dissociative activation of dinitrogen to ammonia over lithium-promoted ruthenium nanoparticles at low pressure. Angew Chem Int Ed 58:17335–17341
86. Zhou Y, Peng X, Zhang T et al (2022) Essential role of Ru–anion interaction in Ru-based ammonia synthesis Catalysts. ACS Catal 12:7633–7642
87. Liu J, Ma X, Li Y et al (2018) Heterogeneous $Fe_3$ single-cluster catalyst for ammonia synthesis via an associative mechanism. Nat Commun 9:1610
88. Wang P, Chang F, Gao W et al (2017) Breaking scaling relations to achieve low-temperature ammonia synthesis through LiH-mediated nitrogen transfer and hydrogenation. Nat Chem 9:64–70
89. Hattori M, Mori T, Arai T et al (2018) Enhanced catalytic ammonia synthesis with transformed BaO. ACS Catal 8:10977–10984
90. Nishi M, Chen S, Takagi H (2019) Mild ammonia synthesis over Ba-promoted Ru/MPC catalysts: effects of the Ba/Ru ratio and the mesoporous structure. Catalysts 9:480–491
91. Shadravan V, Cao A, Bukas VJ et al (2022) Enhanced promotion of Ru-based ammonia catalysts by in situ dosing of Cs. Energy Environ Sci 15:3310–3320
92. Kitano M, Inoue Y, Yamazaki Y et al (2012) Ammonia synthesis using a stable electride as an electron donor and reversible hydrogen store. Nat Chem 4:934–940
93. Lu Y, Li J, Tada T et al (2016) Water durable electride $Y_5Si_3$: Electronic structure and catalytic activity for ammonia synthesis. J Am Chem Soc 138:3970–3973
94. Gong Y, Wu J, Kitano M et al (2018) Ternary intermetallic LaCoSi as a catalyst for $N_2$ activation. Nat Catal 1:178–185
95. Lin B, Fang B, Wu Y et al (2021) Enhanced ammonia synthesis activity of ceria-supported ruthenium catalysts induced by CO activation. ACS Catal 11:1331–1339

96. Zhang X, Liu L, Wu A et al (2022) Synergizing surface hydride species and Ru clusters on $Sm_2O_3$ for efficient ammonia synthesis. ACS Catal 12:2178–2190
97. Zhou Y, Wang J, Liang L et al (2021) Unraveling the size-dependent effect of Ru-based catalysts on ammonia synthesis at mild conditions. J Catal 404:501–511
98. Ogura Y, Sato K, Miyahara SI et al (2018) Efficient ammonia synthesis over a $Ru/La_{0.5}Ce_{0.5}O_{1.75}$ catalyst pre-reduced at high temperature. Chem Sci 9:2230–2237
99. Chang F, Guan Y, Chang X et al (2018) Alkali and alkaline earth hydrides-driven $N_2$ activation and transformation over Mn nitride catalyst. J Am Chem Soc 140:14799–14806
100. Ye T, Park S, Lu Y et al (2020) Vacancy-enabled $N_2$ activation for ammonia synthesis on an Ni-loaded catalyst. Nature 583:391–395
101. Ye T, Park S, Lu Y et al (2020) Contribution of nitrogen vacancies to ammonia synthesis over metal nitride catalysts. J Am Chem Soc 142:14374–14383
102. Honkala K, Hellman A, Remediakis IN et al (2005) Ammonia synthesis from first-principles calculations. Science 307:555–558
103. Li L, Jiang Y, Zhang T et al (2022) Size sensitivity of supported Ru catalysts for ammonia synthesis: From nanoparticles to subnanometric clusters and atomic clusters. Chem 8:749–768
104. Wang Y, Craven M, Yu X et al (2019) Plasma-enhanced catalytic synthesis of ammonia over a $Ni/Al_2O_3$ catalyst at near-room temperature: insights into the importance of the catalyst surface on the reaction mechanism. ACS Catal 9:10780–10793
105. Winter LR, Ashford B, Hung J et al (2020) Identifying surface reaction intermediates in plasma catalytic ammonia synthesis. ACS Catal 10:14763–14774
106. Rouwenhorst KHR, Burbach HGB, Vogel DW et al (2021) Plasma-catalytic ammonia synthesis beyond thermal equilibrium on Ru-based catalysts in non-thermal plasma. Catal Sci Technol 11:2834–2843
107. Carreon ML (2019) Plasma catalytic ammonia synthesis: state of the art and future directions. J Phys D: Appl Phys 52:483001
108. Wang X, Wang W, Qiao M et al (2018) Atomically dispersed $Au_1$ catalyst towards efficient electrochemical synthesis of ammonia. Sci Bull 63:1246–1253
109. Liao W, Qi L, Wang Y et al (2021) Interfacial engineering promoting electrosynthesis of ammonia over Mo/phosphotungstic acid with high performance. Adv Funct Mater 31:2009151–2009159
110. Liu H, Hai G, Ding L et al (2023) Fluorine-stabilized defective black phosphorene as a lithium-like catalyst for boosting nitrogen electroreduction to ammonia. Angew Chem Int Ed 62:e202302124
111. Suryanto BHR, Matuszek K, Choi J et al (2021) Nitrogen reduction to ammonia at high efficiency and rates based on a phosphonium proton shuttle. Science 372:1187–1191
112. Fu X, Pedersen JB, Zhou Y et al (2023) Continuous-flow electrosynthesis of ammonia by nitrogen reduction and hydrogen oxidation. Science 379:707–712
113. Han Q, Jiao H, Xiong L et al (2021) Progress and challenges in photocatalytic ammonia synthesis. Mat Adv 2:564–581
114. Schrauzer GN, Guth TD (1977) Photolysis of water and photoreduction of nitrogen on titanium dioxide. J Am Chem Soc 99:7189–7193
115. Zhao Y, Zhao Y, Shi R et al (2019) Tuning oxygen vacancies in ultrathin $TiO_2$ nanosheets to boost photocatalytic nitrogen fixation up to 700 nm. Adv Mater 31:e1806482
116. Li H, Shang J, Ai ZH et al (2015) Efficient visible light nitrogen fixation with BiOBr nanosheets of oxygen vacancies on the exposed 001 facets. J Am Chem Soc 137:6393–6399
117. Brown KA, Harris DF, Wilker MB et al (2016) Light-driven dinitrogen reduction catalyzed by a CdS: nitrogenase MoFe protein biohybrid. Science 352:448–450
118. Banerjee A, Yuhas BD, Margulies EA et al (2015) Photochemical nitrogen conversion to ammonia in ambient conditions with FeMoS-chalcogels. J Am Chem Soc 137:2030–2034
119. Zhao Y, Zhao Y, Waterhouse GIN et al (2017) Layered-double-hydroxide nanosheets as efficient visible-light-driven photocatalysts for dinitrogen fixation. Adv Mater 29:1703828–1703837
120. Yin H, Chen Z, Peng Y et al (2022) Dual active centers bridged by oxygen vacancies of ruthenium single-atom hybrids supported on molybdenum oxide for photocatalytic ammonia synthesis. Angew Chem Int Ed 61:e2021142
121. Xiong Y, Li B, Gu Y et al (2023) Photocatalytic nitrogen fixation under an ambient atmosphere using a porous coordination polymer with bridging dinitrogen anions. Nat Chem 15:286–293
122. Ammonia market size, share & COVID-19 impact analysis, by application (fertilizers, textile, refrigeration, pharmaceutical, household & industrial cleaning, and others), and regional forecast 2021—2028. https://www.fortunebusinessinsights.com/industry- reports/ammonia-market-101716. Accessed 01 June 2023
123. Intelligence M (2021) ammonia market - growth, trends, COVID-19 Impact, and Forecasts (2021—2026). https://www.reportlinker.com/p06036753/Ammonia-Market- Growth-Trends-COVID-19-Impact-and-Forecasts.html. Accessed 21 May 2023
124. Yara (2018) Yara fertilizer industry handbook
125. Technology roadmap-energy and GHG reductions in the chemical industry via catalytic processes. https://www.iea.org/reports/technology-roadmap-energy-and-ghg-reductions-in- the-chemical-industry-via-catalytic-processes. Accessed 27 May 2023
126. Zweifel T, Naubron J, Grützmacher H (2009) Catalyzed dehydrogenative coupling of primary alcohols with water, methanol, or amines. Angew Chem Int Ed 121:567–571
127. Yamaguchi K, Kobayashi H, Wang Y et al (2013) Green oxidative synthesis of primary amides from primary alcohols or aldehydes catalyzed by a cryptomelane-type manganese oxide-based octahedral molecular sieve, OMS-2. Catal Sci Technol 3:318–327
128. Wang Y, Zhu D, Tang L et al (2011) Highly efficient amide synthesis from alcohols and amines by virtue of a water-soluble gold/DNA catalyst. Angew Chem Int Ed 50:8917–8921
129. Soulé J, Miyamura H, Kobayashi S (2011) Powerful amide synthesis from alcohols and amines under aerobic conditions catalyzed by gold or gold/iron, -nickel or -cobalt nanoparticles. J Am Chem Soc 133:18550–18553
130. Kretschmer R, Schlangen M, Schwarz H (2013) C-N coupling in the gas-phase reactions of ammonia and $[M(CH)]^+$ (M = Ni, Pd, Pt): a combined experimental/computational exercise. Dalton Trans 42:4153–4162
131. Kim J, Kim HJ, Chang S (2013) Synthetic uses of ammonia in transition-metal catalysis. Eur J Org Chem 2013:3201–3213
132. The Potential Future for Ammonia Market Nexus. https://www.ammoniaenergy.org/ paper/the-potential-future-for-ammonia-market-nexus. Accessed 05 June 2023
133. Luo Y, Liang S, Wang X et al (2022) Facile synthesis and high-value utilization of ammonia. Chinese J Chem 40:953–964
134. Boisen A, Dahl S, Norskov J et al (2005) Why the optimal ammonia synthesis catalyst is not the optimal ammonia decomposition catalyst. J Catal 230:309–312
135. Tsai W, Weinberg WH (1987) Steady-state decomposition of ammonia on the ruthenium(001) surface. J Phys Chem 91:5302–5307
136. Takahashi A, Fujitani T (2016) Kinetic analysis of decomposition of ammonia over nickel and ruthenium catalysts. J Chem Eng Japan 49:22–28
137. Schüth F, Palkovits R, Schlögl R et al (2012) Ammonia as a possible element in an energy infrastructure: catalysts for ammonia decomposition. Energy Environ Sci 5:6278–6289
138. Le TA, Do QC, Kim Y et al (2021) A review on the recent developments of ruthenium and nickel catalysts for $CO_x$-free $H_2$ generation by ammonia decomposition. Korean J Chem Eng 38:1087–1103
139. Lamb K, Hla SS, Dolan M (2019) Ammonia decomposition kinetics over LiOH-promoted, $\alpha$-$Al_2O_3$-supported Ru catalyst. Int J Hydrog Energy 44:3726–3736
140. Cha J, Lee T, Lee Y et al (2021) Highly monodisperse sub-nanometer and nanometer Ru particles confined in alkali-exchanged zeolite Y for ammonia decomposition. Appl Catal B 283:119627
141. Fang H, Wu S, Ayvali T et al (2023) Dispersed surface Ru ensembles on MgO(111) for catalytic ammonia decomposition. Nat Commun 1:647
142. Ogasawara K, Nakao T, Kishida K et al (2021) Ammonia decomposition over CaNH-supported Ni catalysts via an $NH^{2-}$-vacancy-mediated Mars–van Krevelen mechanism. ACS Catal 11:11005–11015
143. Do QC, Kim Y, Le TA et al (2022) Facile one-pot synthesis of Ni-based catalysts by cation-anion double hydrolysis method as highly active Ru-free catalysts for green $H_2$ production via $NH_3$ decomposition. Appl Catal B 307:121167
144. Su T, Guan B, Zhou J et al (2023) Review on Ru-based and ni-based catalysts for ammonia decomposition: research status, reaction mechanism, and perspectives. Energy Fuels 37:8099–8127

145. Zhang LF, Li M, Ren TZ et al (2015) Ce-modified Ni nanoparticles encapsulated in $SiO_2$ for $CO_x$-free hydrogen production via ammonia decomposition. Int J Hydrogen Energy 40:2648–2656
146. Okura K, Okanishi T, Muroyama H et al (2016) Ammonia decomposition over nickel catalysts supported on rare-earth oxides for the on-site generation of hydrogen. ChemCatChem 8:2988–2995
147. Fang H, Zhou Y, Peng X et al (2023) Challenges and prospects in artificial nitrogen cycle for energy decarbonization. Natl Sci Open 2:20220040
148. Lin L, Zhang L, Luo Y et al (2022) Highly-integrated and cost-efficient ammonia-fueled fuel cell system for efficient power generation: a comprehensive system optimization and techno-economic analysis. Energy Convers Manag 251:114917
149. Zhang H, Zhou Y, Pei K et al (2022) An efficient and durable anode for ammonia protonic ceramic fuel cells. Energy Environ Sci 15:287–295
150. Li Y, Pillai HS, Wang T et al (2021) High-performance ammonia oxidation catalysts for anion-exchange membrane direct ammonia fuel cells. Energy Environ Sci 14:1449–1460
151. Meng G, Jiang C, Ma J et al (2007) Comparative study on the performance of a SDC-based SOFC fueled by ammonia and hydrogen. J Power Sources 173:189–193
152. Aoki Y, Yamaguchi T, Kobayashi S et al (2018) High-efficiency direct ammonia fuel cells based on $BaZr_{0.1}Ce_{0.7}Y_{0.2}O_{3-\delta}$/Pd oxide-metal junctions. Global Challenges 2:1700088
153. He F, Gao Q, Liu Z et al (2021) A new Pd doped proton conducting perovskite oxide with multiple functionalities for efficient and stable power generation from ammonia at reduced temperatures. Adv Energy Mater 11:2003916
154. Fang H, Cheng J, Luo Y et al (2022) Progress of ammonia electrooxidation catalyst and its performance in low temperature direct ammonia alkaline membrane fuel cell. CIESC J 73:3802–3814
155. Elbaz AM, Wang S, Guiberti TF et al (2022) Review on the recent advances on ammonia combustion from the fundamentals to the applications. Fuel Commun 10:100053
156. Kobayashi H, Hayakawa A, Somarathne KDKA et al (2019) Science and technology of ammonia combustion. Proc Combust Inst 37:109–133
157. Kurata O, Iki N, Matsunuma T et al (2017) Performances and emission characteristics of $NH_3$–air and $NH_3CH_4$–air combustion gas-turbine power generations. Proc Combust Inst 36:3351–3359
158. Da Rocha RC, Costa M, Bai X (2019) Chemical kinetic modelling of ammonia/hydrogen/air ignition, premixed flame propagation and NO emission. Fuel 246:24–33
159. Goldmann A, Dinkelacker F (2018) Approximation of laminar flame characteristics on premixed ammonia/hydrogen/nitrogen/air mixtures at elevated temperatures and pressures. Fuel 224:366–378
160. Ichikawa A, Hayakawa A, Kitagawa Y et al (2015) Laminar burning velocity and markstein length of ammonia/hydrogen/air premixed flames at elevated pressures. Int J Hydrog Energy 159:98–106
161. Okafor EC, Naito Y, Colson S et al (2019) Measurement and modelling of the laminar burning velocity of methane-ammonia-air flames at high pressures using a reduced reaction mechanism. Combust Flame 204:162–175
162. Li R, Konnov AA, He G et al (2019) Chemical mechanism development and reduction for combustion of $NH_3/H_2/CH_4$ mixtures. Fuel 257:116059
163. Han X, Wang Z, Costa M et al (2019) Experimental and kinetic modeling study of laminar burning velocities of $NH_3$/air, $NH_3/H_2$/air, $NH_3$/CO/air and $NH_3/CH_4$/air premixed flames. Combust Flame 206:214–226
164. Okafor EC, Naito Y, Colson S et al (2018) Experimental and numerical study of the laminar burning velocity of $CH_4$–$NH_3$–air premixed flames. Combust Flame 187:185–198
165. Wang S, Wang Z, Chen C et al (2022) Applying heat flux method to laminar burning velocity measurements of $NH_3/CH_4$/air at elevated pressures and kinetic modeling study. Combust Flame 236:111788
166. Ichikawa A, Naito Y, Hayakawa A et al (2019) Burning velocity and flame structure of $CH_4/NH_3$/air turbulent premixed flames at high pressure. Int J Hydrog Energy 44:6991–6999
167. Chen Z, Jiang Y (2021) Numerical investigation of the effects of $H_2$/CO/syngas additions on laminar premixed combustion characteristics of $NH_3$/air flame. Int J Hydrog Energy 46:12016–12030
168. Han X, Wang Z, He Y et al (2020) Experimental and kinetic modeling study of laminar burning velocities of $NH_3$/syngas/air premixed flames. Combust Flame 213:1–13
169. Wang Z, Han X, He Y et al (2021) Experimental and kinetic study on the laminar burning velocities of $NH_3$ mixing with $CH_3OH$ and $C_2H_5OH$ in premixed flames. Combust Flame 229:111392
170. Elbaz AM, Giri BR, Issayev G et al (2020) Experimental and kinetic modeling study of laminar flame speed of dimethoxymethane and ammonia blends. Energy Fuels 34:14726–14740
171. Issayev G, Giri BR, Elbaz AM et al (2022) Ignition delay time and laminar flame speed measurements of ammonia blended with dimethyl ether: a promising low carbon fuel blend. Renew Energ 181:1353–1370
172. Issayev G, Giri BR, Elbaz AM et al (2021) Combustion behavior of ammonia blended with diethyl ether. Proc Combust Inst 38:499–506
173. Wang D, Ji C, Wang Z et al (2020) Measurement of oxy-ammonia laminar burning velocity at normal and elevated temperatures. Fuel 279:118425
174. Karan A, Dayma G, Chauveau C et al (2022) Experimental study and numerical validation of oxy-ammonia combustion at elevated temperatures and pressures. Combust Flame 236:111819
175. Shrestha KP, Lhuillier C, Barbosa AA et al (2021) An experimental and modeling study of ammonia with enriched oxygen content and ammonia/hydrogen laminar flame speed at elevated pressure and temperature. Proc Combust Inst 38:2163–2174
176. Xia Y, Hashimoto G, Hadi K et al (2020) Turbulent burning velocity of ammonia/oxygen/nitrogen premixed flame in $O_2$-enriched air condition. Fuel 268:117383
177. Wang S, Elbaz AM, Wang Z et al (2021) The effect of oxygen content on the turbulent flame speed of ammonia/oxygen/nitrogen expanding flames under elevated pressures. Combust Flame 232:111521
178. He X, Shu B, Nascimento D et al (2019) Auto-ignition kinetics of ammonia and ammonia/hydrogen mixtures at intermediate temperatures and high pressures. Combust Flamee 206:189–200
179. Okafor EC, Yamashita H, Hayakawa A et al (2021) Flame stability and emissions characteristics of liquid ammonia spray co-fired with methane in a single stage swirl combustor. Fuel 287:119433
180. Franco MC, Rocha RC, Costa M et al (2021) Characteristics of $NH_3/H_2$/air flames in a combustor fired by a swirl and bluff-body stabilized burner. Proc Combust Inst 38:5129–5138
181. Khateeb AA, Guiberti TF, Zhu X et al (2020) Stability limits and NO emissions of technically-premixed ammonia-hydrogen-nitrogen-air swirl flames. Int J Hydrog Energy 45:22008–22018
182. Khateeb AA, Guiberti TF, Wang G et al (2021) Stability limits and NO emissions of premixed swirl ammonia-air flames enriched with hydrogen or methane at elevated pressures. Int J Hydrog Energy 46:11969–11981
183. Okafor EC, Somarathne KDKA, Hayakawa A et al (2019) Towards the development of an efficient low-$NO_x$ ammonia combustor for a micro gas turbine. Proc Combust Inst 37:4597–4606
184. Okafor EC, Somarathne KDKA, Ratthanan R et al (2020) Control of $NO_x$ and other emissions in micro gas turbine combustors fuelled with mixtures of methane and ammonia. Combust Flame 211:406–416
185. Zhu X, Khateeb AA, Guiberti TF et al (2021) NO and OH emission characteristics of very-lean to stoichiometric ammonia–hydrogen–air swirl flames. Proc Combust Inst 38:5155–5162
186. Khateeb AA, Guiberti TF, Zhu X et al (2020) Stability limits and exhaust NO performances of ammonia-methane-air swirl flames. Exp Therm Fluid Sci 114:110058
187. Zhang J, Cao Y, Ding F et al (2023) Few-layered hexagonal boron nitrides as highly effective and stable solid adsorbents for ammonia separation. Ind Eng Chem Res 62:3705–3715
188. Cao Y, Zhang J, Ma Y et al (2021) Designing low-viscosity deep eutectic solvents with multiple weak-acidic groups for ammonia separation. ACS Sustain Chem Eng 9:7352–7360


## Publisher's Note